Available online at www.sciencedirect.com
SCIENCE DIRECT®
Geochimica et Cosmochimica Acta 70 (2006) 1356–1378
Geochimica
www.elsevier.com/locate/gca

Incorporating solid solutions in reactive transport equations using a kinetic discrete-composition approach

Peter C. Lichtner *, J. William Carey

LANL EES-6: MS D469, Los Alamos National Laboratory, SM-30 Bikini Atoll Road, Los Alamos, NM 87545, USA

Received 1 August 2005; accepted in revised form 21 November 2005

Abstract

A new approach is proposed for incorporating solid solution reactions into mass conservation equations describing reaction paths in both closed and open systems. The method is applicable to problems involving advective, dispersive, and diffusive transport in a porous medium. By representing the continuously variable solid solution composition with a discrete set of stoichiometric solids that span composition space, combined with a kinetic formulation of their rates of reaction, a self-determining spatial and temporal evolution of the solid solution concentration and composition is obtained. It is demonstrated that equilibrium of an aqueous solution with a stoichiometric solid derived from a solid solution corresponds to equilibrium of the solid solution itself if and only if equilibrium of the stoichiometric solid is stable. One advantage of this approach is that it is unnecessary to introduce any additional compositional variables to represent the solid solution. Discretization may be over the entire range of composition space, or over some subset depending on the system. A major consequence of the kinetic discrete-composition solid solution representation is that modeling solid solutions is similar to modeling pure mineral phases with the exception of a weighting factor applied to reaction rates of stoichiometric solids corresponding to a common solid solution. With this approach, precipitation leads to a discrete zonation of the solid solution that approximates the continuous variation in composition expected for the actual solid solution. The approach is demonstrated for a hypothetical ideal and non-ideal binary solid solution $A_xB_{1-x}C$ for a reaction path formulation and reactive transport involving advection and diffusion.

1. Introduction

Solid solutions are ubiquitous rock-forming minerals and are essential for understanding many geological processes. For example, a recent study of hydrothermal ore-forming processes of silver in the Coeur d'Alene mining district in northern Idaho led to the development of a thermodynamic model for Ag–Cu solid solution in fahore and Fe–Zn in sphalerite and provided an extensive database for sulfide and sulfosalt solid solutions (Sack et al., 2005; Sack, 2005). In a study of crustal metamorphism of carbonates, Ferry et al. (2005) concluded that solid solutions were needed to explain field observations of layered carbonation-decarbonation reactions at Val d'Efra, Central Alps, Switzerland.

In spite of the obvious importance of solid solutions in fluid–rock interactions, little progress has been made to couple these reactions to transport equations describing advection, dispersion, and diffusion. In part, this may be due to the inherent complexity that can result from reactions involving solid solutions. Although congruent dissolution of a solid solution with fixed composition can be described in a similar fashion to dissolution of a stoichiometric mineral, precipitation and dissolution/recrystallization processes are much more complex (Murphy and Smith, 1988; Glynn and Reardon, 1990). This is a direct consequence of the continuously variable composition of a solid solution. Consider an aqueous solution that is supersaturated with some solid solution forming mineral. As precipitation commences, a range of compositions can form depending on reaction kinetics of the solid solution.

* Corresponding author. Fax: +1 505 665 3285.
E-mail addresses: lichtner@lanl.gov (P.C. Lichtner), bcarey@lanl.gov (J.W. Carey).

0016-7037/$ - see front matter © 2005 Elsevier Inc. All rights reserved.
doi:10.1016/j.gca.2005.11.028

List of symbols

A	Chemical species [—]
$\mathcal{A}_j$	The jth primary species [—]
$A_{x_{mk}}$	Specific surface area of discretized stoichiometric solid with composition x_{mk} [m^{-1}]
AC	Binary solid solution end member [—]
a_1, a_2	Binary solid solution activities [—]
a_{A^+}, a_{B^+}, a_{C^-}	Activities of species A^+, B^+, and C^- [—]
a_i^m	Solid activity of the ith end member in the mth solid solution [—]
B	Chemical species [—]
BC	Binary solid solution end member [—]
C	Chemical species [—]
D	Diffusion/dispersion coefficient [m^2/s]
$\mathbf{F}_{A^+}$, $\mathbf{F}_{B^+}$, $\mathbf{F}_{C^-}$	Fluxes of species A^+, B^+, and C^- [mol/m^2/s]
$\mathcal{F}_{x_{mk}}$	Rate factor to control reversibility [—]
G_M	Gibbs free energy of solid solution mixture [J/mol]
$I_{x_{mk}}$	Kinetic reaction rate for the discretized stoichiometric solid with composition x_{mk} [mol/m^3/s]
K_i^{aq}	Equilibrium constant for the ith secondary species [—]
K_i^m	Equilibrium constant of the ith end member in the mth solid solution [—]
K_{x_m}, $K_{x_{mk}}$	Equilibrium constant for stoichiometric solid with composition x_m and discretized form x_{mk} [—]
K_{ss}	Stoichiometric solid equilibrium constant for a binary solid solution [—]
K_1, K_2	Binary solid solution equilibrium constants [—]
$k_{x_{mk}}$	Kinetic rate constant for discretized stoichiometric solid with composition x_{mk} [mol/m^2/s]
$\mathcal{L}_m$	Solidus for the mth solid solution [—]
l_m	Solutus for the mth solid solution [—]
$\mathcal{M}_i^m$	The ith end member of the mth solid solution [—]
m_i	Molality of the ith secondary species [mol/kg H_2O]
m_j	Molality of the jth primary species [mol/kg H_2O]
m_{A^+}, m_{B^+}, m_{C^-}	Molality of species A^+, B^+, and C^- [mol/kg H_2O]
N_c	Number of aqueous primary species [—]
N_m	Number of end members in the mth solid solution [—]
$N_R^{\pm}$	Number of precipitating (+) and dissolving (−) stoichiometric solids belonging to a solid solution in a control volume [—]
p	Pressure [Pa]
Q_i^m	Ion activity product of the ith end member in the mth solid solution [—]
Q_{x_m}	Ion activity product of stoichiometric solid with composition x_m [—]
Q_{ss}	Ion activity product of stoichiometric solid for a binary solid solution [—]
$\mathbf{q}$	Darcy velocity [m/s]
R	Gas constant [mol/J/K]
$\mathbf{r}$	3D spatial coordinate [m]
S_i^m	Saturation state of ith end member of the mth solid solution [—]
S_{x_m}, $S_{x_{mk}}$	Saturation for stoichiometric solid with composition x_m and discretized form x_{mk} [—]
S_{ss}	Saturation for stoichiometric solid for a binary solid solution [—]
S_1, S_2	Saturation state for binary solid solution end members [—]
S_m^*	Common saturation point of end members and stoichiometric solid solution [—]
T	Temperature [°C]
t	Time [s]
$\overline{V}_{x_{mk}}$	Molar volume for the discretized solid solution with composition x_{mk} [m^3/mol]
$\overline{V}_{ss}$	Molar volume for the stoichiometric solid in a binary solid solution [m^3/mol]
x_i^m	Mole fraction of ith end member in the mth solid solution [—]
x_m	N_m—tuple $(x_1^m, \ldots, x_{N_m}^m)$ mole fractions of end members in the mth solid solution [—]
x_{mk}	N_m—tuple $(x_{1k_1}^m, \ldots, x_{N_m k_{Z_m}}^m)$ mole fractions of end members in the mth discretized solid solution [—]
x	Composition variable for binary solid solution ($x = x_1$) [—]
Z_m	Total number of discrete stoichiometric solids for the mth solid solution [—]
Z_i^m	Total number of discrete stoichiometric solids for the ith end member of the mth solid solution [—]
α_0, α_1	Guggenheim parameters [—]
$\gamma_{j,i}$	Activity coefficient of the jth primary species or ith secondary species [kg H_2O/L]
δ_{il}	Kronecker delta function [—]
$\zeta_{x_{mk}}$	Rate factor [—]
λ_i^m	Activity coefficient of the ith end member in the mth solid solution [—]
λ_1, λ_2	Activity coefficients for a binary solid solution [—]

μ_i^m	Chemical potential of ith end member in the mth solid solution [J/mol]	τ	Tortuosity [—]
μ_1, μ_2	Chemical potentials of end members in binary solid solution [J/mol]	φ	Porosity [—]
ν_{ji}^m	Stoichiometric solid reaction matrix for the ith end member in the mth solid solution [—]	$\varphi_{x_{mk}}$	Volume fraction for stoichiometric solid solution with composition x_{mk} [—]
ν_{ji}^{aq}	Stoichiometric reaction matrix for homogeneous aqueous reactions [—]	φ_{ss}	Volume fraction for stoichiometric binary solid solution [—]
$\widetilde{\nu}_{jm}$	Stoichiometric coefficient matrix for the overall stoichiometric solid solution [—]	Ψ_j	Total concentration of the jth primary species [mol/L]
ρ_{f}	Fluid density [kg/m^3]	$\boldsymbol{\Omega}_j$	Total flux of the jth primary species [mol/m^2/s]
σ	Scale factor [—]	$\omega_{x_{mk}}$, ω_k	Weight factor for kinetic reaction rate [—]
		$\langle\cdots\rangle$	Mean composition value [—]

As the aqueous solution evolves over time, other compositions become supersaturated and may precipitate. Subsequent precipitates are generally not in equilibrium with previous precipitates which therefore must dissolve. In this way, both the solid and aqueous solution compositions become altered until equilibrium is achieved (possibly involving very long times) at some unique solid and aqueous solution compositions. Surface armoring may prevent recrystallization of the solid solution and the system can behave irreversibly with the development of compositionally zoned minerals. In a system involving advective and diffusive transport the situation is even more complicated. In such cases it is possible to form a solid solution with a spatially variable composition from an initial homogeneously distributed solid solution with fixed composition. Recrystallization in response to changing fluid composition can range from irreversible reaction with no recrystallization, to complete recrystallization.

Murphy and Smith (1988) developed an irreversible kinetic model for solid solution reaction in which they assumed that dissolution proceeded from a single stoichiometric phase with zero order kinetics. They treated precipitation by assuming that the most stable solid composition formed. Back reaction of precipitated secondary phases was prohibited. Glynn et al. (1990) presented a model for calculating reaction paths involving reversible and irreversible reaction with solid solutions using the approach introduced by Helgeson (1968) for describing changes in geochemical systems in partial equilibrium. In this approach, mass action equations for each solid solution end member (or component) are imposed on the system together with mass conservation equations that provide an equal number of equations as unknowns for the aqueous composition and a unique solid solution composition and abundance. Irreversible processes are incorporated in the model by removing mass from the system thereby preventing back reaction. As noted by Glynn et al. (1990), however, the actual path followed by the system is controlled by reaction kinetics. They applied their model to both Berthelot–Nernst and Doerner–Hoskins limiting cases of solid solution precipitation. The Berthelot–Nernst case corresponds to completely reversible reaction in which the solid solution re-equilibrates with the fluid. The Doerner–Hoskins case, by contrast, assumes complete irreversibility of secondary products, which are assumed to become armored and thereby isolated from the fluid so that back reaction does not occur. The final state of this case thus depends on the reaction path. Several computer codes implement an equilibrium formulation of reactions involving solid solutions (Parkhurst and Appelo, 1999; Wolery, 1992); however, such models would appear to have limited applicability due to their neglect of kinetics. In the PHREEQEC code (Parkhurst and Appelo, 1999), it is assumed that for each time step a solid solution dissolves entirely and reprecipitates in equilibrium with the solution. Recently, Nourtier-Mazauric et al. (2005) presented a kinetic model for describing reaction of ideal solid solutions in a batch reactor. In their formulation only the most stable phase is allowed to precipitate.

It should be remarked that an argument often put forward to justify the use of local equilibrium for mineral reaction rates is that kinetic rate laws and their associated rate constants and surface areas are not well established. However, this deficiency would not appear to justify taking the rate constant to be infinite rather than some finite value. Qualitatively different behavior is obtained for finite versus infinite kinetics: for example, the finite time associated with formation of an advancing reaction front in a kinetic description. While some problems may be adequately characterized by the local equilibrium assumption, many mineral–fluid interactions are characterized by sluggish mineral reactions. The kinetic formulation enables both of these cases to be considered in a single framework with local equilibrium obtained as a special case of the kinetic description. Kinetics has the advantage of being more flexible, allowing the departure from local equilibrium to be investigated even if the precise form of the rate law is unknown.

In this work, a new approach is introduced for incorporating solid solutions into multicomponent reactive transport equations by discretizing the solid solution into a finite set of stoichiometric solids with fixed compositions. Central to this formulation is a kinetic description of solid

solution reaction rates. With this approach it is demonstrated that the solid solution composition is self determined both spatially and temporally from the reactive transport equations, without the necessity to introduce any additional composition variables. In this sense, the treatment of solid solutions is no different than that of a pure phase. The advantage of a kinetic formulation is that not only are mineral concentrations determined directly from mass conservation equations, but also the solid solution composition.

In the following, we first develop the general analytical equations for calculating solid-solution equilibria and the relation between end-member and stoichiometric composition equilibria (Sections 2.1 and 2.2). We then develop the discrete approximation and its implementation in reaction path and transport equations (Sections 2.3–2.5). Finally, an example binary solid solution is used to illustrate the discrete model and demonstrate that it accurately approximates analytical results (Section 3).

2. General relations

The usual approach to describe the reaction of pure solid phases in reactive transport equations is to introduce variables for the concentration or abundance of each phase as a function of time and space. A solution to the governing equations provides both the region in space occupied by each solid and its mineral abundance at each grid point. The implementation of a kinetic description of mineral reactions, besides being more realistic, also has an important numerical advantage. It allows the solid evolution over a single time step to be approximately decoupled from equations describing the evolution of the aqueous solution through an operator splitting approach. This decoupling depends on the slow changes in properties of the porous medium resulting in a quasi-stationary behavior (Lichtner, 1988). Thus over a time step, first the solid concentrations, their surface areas, and porosity are frozen in place and only the fluid composition is allowed to change. Solving for the new fluid composition provides both solute concentrations at the new time step and mineral reaction rates. Once the mineral reaction rates have been obtained, new mineral concentrations follow by integrating the mineral mass transfer equations over the time step. In this way, the reacting mineral assemblage at each location in the computational domain is directly determined from the transport equations without the need for any further analysis. It is essential, of course, to include the correct set of reacting minerals and exclude those minerals which thermodynamically may be possible to react, but which are inhibited by nucleation kinetics.

In the case of solid solutions for which composition is continuously variable, the situation becomes much more complex. In this case, the solid solution composition must be determined in addition to its abundance, as they both evolve temporally and spatially with changing solution composition. Thus, incorporation of solid solutions into reactive transport equations would appear to necessitate the introduction of additional descriptive quantities: namely, a set of continuous variables to specify the solid solution composition at as a function of time and space. To make matters even more difficult, complete re-equilibration of the solid solution with the changing aqueous phase may occur only partially or not at all, making it necessary to keep track of different solid solution compositions and abundances through additional degrees of freedom as new layers are deposited at different points in space at different times. This possibility introduces all sorts of complicating effects such as surface armoring with newly deposited layers, etc. In what follows such effects including solid state diffusion are not considered further.

With this caveat, in this work it is demonstrated that the same techniques used for describing the reaction of pure phases in reactive transport equations can also be applied to solid solutions. The approach developed here is to discretize the solid solution composition: a solid solution is represented through a discrete set of compositions that span some subset (which may include the entire range) of composition space sufficient to characterize the particular system at hand. This approach thus circumvents the need to solve for additional composition variables. In order to accurately represent changes in composition, a sufficiently fine compositional discretization of the solid solution must be used. In this way, a continuous variation in composition is replaced by a discrete set of compositions. Each solid solution composition is treated as a stoichiometric solid. All such solids are governed by a kinetic rate law and may be considered to react reversibly or irreversibly. Because of the kinetic nature of the solid solution reaction rates, more than one solid composition is generally present at any given location and at any particular time. As shown below for reaction path simulations, the kinetic implementation drives the stoichiometric solid solution system to its true equilibrium composition. Thus, through a kinetic implementation of mineral reaction rates combined with a discrete set of solid solution compositions, a seamless approach to incorporating solid solutions into reactive transport equations is achieved without the introduction of additional composition variables.

2.1. Solid solutions

Reaction of the mth solid solution whose composition is represented symbolically by $(\mathcal{M}_1^m)_{x_1^m}(\mathcal{M}_2^m)_{x_2^m}\ldots(\mathcal{M}_{N_m}^m)_{x_{N_m}^m}$, having mole fractions x_i^m of the ith end member $\mathcal{M}_i^m$, with an aqueous solution is described by the simultaneous N_m end-members reactions

$$\sum_j \nu_{ji}^m \mathcal{A}_j \rightleftharpoons \mathcal{M}_i^m \quad (i = 1, \ldots, N_m), \tag{2.1}$$

with aqueous primary species $\mathcal{A}_j$ and stoichiometric reaction coefficients ν_{ji}^m. There are $N_m - 1$ independent solid composition variables due to the constraint

$$\sum_{i=1}^{N_m} x_i^m = 1. \tag{2.2}$$

The shorthand notation x_m is used to denote the N_m-tuple: $x_m = \{x_1^m, \ldots, x_{N_m}^m\}$, with the following notation for the solid solution chemical formula

$$\mathcal{M}_{x_m} = (\mathcal{M}_1^m)_{x_1^m} (\mathcal{M}_2^m)_{x_2^m} \ldots (\mathcal{M}_{N_m}^m)_{x_{N_m}^m} = \prod_i (\mathcal{M}_i^m)_{x_i^m}. \tag{2.3}$$

Other formulations of solid-solution components besides using end members are also possible such as site occupancy and exchange ions (Nordstrom and Munoz, 1985). However, this does not affect the presentation given here and these other approaches are not considered further. Pure phases in addition to solid solutions can be treated with the same formulation by setting $N_m = 1$.

Equilibrium of a solid solution with an aqueous solution consists of the N_m mass action relations

$$K_i^m = \frac{a_i^m}{Q_i^m} \quad (i = 1, \ldots, N_m), \tag{2.4}$$

with equilibrium constant $K_i^m(T,p)$ a function of temperature T and pressure p, end-member solid activity a_i^m, and ion activity product Q_i^m defined by

$$Q_i^m = \prod_j \left(\gamma_j m_j\right)^{\nu_{ji}^m}, \tag{2.5}$$

where m_j refers to the molality of the jth primary species with activity coefficient γ_j. For an ideal solid solution the activity of the ith end member is equal to its mole fraction

$$a_i^m = x_i^m. \tag{2.6}$$

In the general case of nonideality the solid activity is expressed as

$$a_i^m = \lambda_i^m x_i^m, \tag{2.7}$$

with solid activity coefficient λ_i^m.

The overall reaction of the stoichiometric solid solution with fixed composition x_m is obtained by summing the individual end-member reactions, Eq. (2.1), weighted by their respective mole fractions to give

$$\sum_{ji} x_i^m \nu_{ji}^m \mathcal{A}_j \rightleftharpoons \sum_i x_i^m \mathcal{M}_i^m \rightleftharpoons \mathcal{M}_{x_m}. \tag{2.8}$$

Eq. (2.8) may be rewritten more concisely as

$$\sum_j \widetilde{\nu}_{jm} \mathcal{A}_j \rightleftharpoons \mathcal{M}_{x_m}, \tag{2.9}$$

with

$$\widetilde{\nu}_{jm} = \sum_i \nu_{ji}^m x_i^m. \tag{2.10}$$

The corresponding mass action relation is given by

$$\prod_i (K_i^m)^{x_i^m} = \prod_i \left(\frac{a_i^m}{Q_i^m}\right)^{x_i^m}. \tag{2.11}$$

Defining the equilibrium coefficient K_{x_m} for the stoichiometric solid solution $\mathcal{M}_{x_m}$ in terms of the end-member equilibrium constants and their activities as

$$K_{x_m}(T,p,x_m) = \prod_i \left(\frac{K_i^m}{a_i^m}\right)^{x_i^m}, \tag{2.12}$$

then equilibrium of the stoichiometric solid solution with composition x_m follows as:

$$K_{x_m} Q_{x_m} = 1, \tag{2.13}$$

where the ion activity product Q_{x_m} is given by

$$Q_{x_m} = \prod_i (Q_i^m)^{x_i^m}. \tag{2.14}$$

The equilibrium coefficient K_{x_m} is a function of the composition of the stoichiometric solid in addition to temperature and pressure. The product $K_{x_m} Q_{x_m}$ is defined as the saturation state $S_{x_m}(x_m)$ of the stoichiometric solid solution with composition x_m

$$S_{x_m}(x_m) = K_{x_m} Q_{x_m}, \tag{2.15}$$

$$= \prod_i \left(\frac{K_i^m}{a_i^m} Q_i^m\right)^{x_i^m}. \tag{2.16}$$

It follows that $S_{x_m}(x_m)$ can be expressed as a product of the end-member saturation states according to

$$S_{x_m}(x_m) = \prod_i (S_i^m)^{x_i^m}, \tag{2.17}$$

where S_i^m refers to the saturation state of the ith end member defined as

$$S_i^m = \frac{K_i^m}{a_i^m} Q_i^m. \tag{2.18}$$

As has been noted previously (e.g., Glynn et al., 1990, and others), an aqueous solution that is in equilibrium with the stoichiometric solid solution $\mathcal{M}_{x_m}$ defined by Eq. (2.13), does not imply that it is also in equilibrium with the solid solution itself as defined by Eq. (2.4). Equilibrium with respect to the stoichiometric solid solution alone imposes only one condition on the system, whereas equilibrium with each end member imposes N_m independent conditions given by Eq. (2.4). Thus, equilibrium of an aqueous solution with any particular stoichiometric solid composition is only a necessary but not sufficient condition for equilibrium of the solid solution. To impose equilibrium of the solid solution, N_m conditions are needed: either each end member must satisfy a corresponding equilibrium condition of the form of Eq. (2.4), or equilibrium with $N_m - 1$ end members and one stoichiometric solid solution composition is required.

The above remarks apply to a continuous solid solution. In the presence of a miscibility gap with the coexistence of several phases, it is necessary to augment the above formulation with the equality of the chemical potentials in the different phases (e.g., Prigogine and Defay, 1969). Coexistence of the exsolved phases implies the equilibrium relations

$$\mu_i^m = (\mu_i^m)', \tag{2.19}$$

where μ_i^m and $(\mu_i^m)'$ refer to the chemical potentials of the end members with compositions x_m and x'_m, respectively,

leading to additional constraints for equilibrium of the solid solution.

2.2. Stability

To make use of the numerical advantages afforded by pure solid phases, the continuously variable composition solid solution is replaced by a discrete set of stoichiometric solids. However, for this approach to be meaningful, it must first be demonstrated that such a system can correctly represent equilibrium states of a solid solution interacting with an aqueous fluid. Stability is the key for understanding the relation between equilibrium of a stoichiometric solid and equilibrium of its corresponding solid solution.

An equilibrium point is stable, if the first partial derivatives of the saturation with respect to changes in composition vanishes, and for a binary solid solution the second derivative is negative [more complicated criteria exists for multicomponent solid solutions derived by Prigogine and Defay (1969)]. We demonstrate that equilibrium of a stoichiometric solid solution implies equilibrium of the solid solution if and only if the stoichiometric solid is in a stable equilibrium state. To accomplish this, note that if a common saturation state S_m^* exists among end members, so that

$$S_1^m = S_2^m = \cdots = S_{N_m}^m = S_m^*, \tag{2.20}$$

then the stoichiometric solid solution with composition x_m also has the same saturation state

$$S_{x_m} = \prod_i (S_m^*)^{x_i^m} = (S_m^*)^{\sum_i x_i^m} = S_m^*. \tag{2.21}$$

Thus, if all end-member saturation states are equal to each other, they are equal to the stoichiometric solid solution saturation. In particular, if $S_m^* = 1$, then since the end members are in equilibrium, the solid solution with composition x_m is in equilibrium as is the stoichiometric solid with the same composition.

Furthermore, at the common intersection point of the end members and stoichiometric solid saturation curves, the stoichiometric saturation state is at an extremum, and conversely. This observation follows from the relation (see Appendix A)

$$\frac{\partial}{\partial x_l} \ln S_{x_m}\bigg|_{S_m^*} = \ln\left(\frac{S_l^m}{S_{N_m}^m}\right)\bigg|_{S_m^*} = 0, \tag{2.22}$$

and thus the first derivative of the stoichiometric saturation vanishes at the common intersection point S_m^*. Conversely, if the first derivative of the stoichiometric saturation with respect to all end members vanishes, then the point at which it vanishes must be a common saturation point. To determine whether the extremum is a minimum, maximum, or inflection point, the second derivative is needed, given by

$$\frac{\partial^2}{\partial x_i^m \partial x_l^m} \ln S_{x_m}\bigg|_{S_m^*} = -\frac{x_i^m + \delta_{il} x_{N_m}^m}{x_i^m x_{N_m}^m} - \frac{\partial}{\partial x_l^m} \ln\left(\frac{\lambda_i^m}{\lambda_{N_m}^m}\right), \tag{2.23}$$

where δ_{il} denotes the Kronecker delta function. For a binary solid solution with $x = x_1^m$ this expression reduces to

$$\frac{\partial^2}{\partial x^2} \ln S_{x_m}\bigg|_{S_m^*} = -\frac{1}{x(1-x)} - \frac{\partial}{\partial x} \ln\left(\frac{\lambda_1}{\lambda_2}\right). \tag{2.24}$$

For an ideal solution the second derivative at the common intersection point is always negative, implying the extremum is always a maximum and thus equilibrium of the solid solution is always stable. Thus, for an ideal solid solution, an equilibrium point of a stoichiometric solid solution is stable if and only if it is a true equilibrium state of the solid solution. It follows in this case that if the stoichiometric solid is in equilibrium for some particular composition, but the solid solution is not in equilibrium, then the equilibrium point must be unstable. In this case, according to Eq. (2.22), the first derivative does not vanish and neighboring compositions are supersaturated or undersaturated. As a consequence, reaction must continue until the system achieves a stable equilibrium state. Because over the range of stoichiometric solid compositions the only stable equilibrium state is true equilibrium of the solid solution, and if essentially all possible solid compositions are available to react, the system can "find" the true equilibrium state and thus cannot become trapped in an unstable state representing false equilibrium.

These relations are depicted in Figs. 1a and b for an ideal binary solid solution of the form $A_xB_{1-x}C$, in which the stoichiometric saturation $S(x)$ [Eq. (2.16)], and end-member saturations $S_1(x)$ and $S_2(x)$ [Eq. (2.18)] are plotted as a function of composition x to illustrate stable and unstable equilibrium conditions (see Section 3.1.1 below for parameters used to generate the figures). In Fig. 1a, a solution composition in true equilibrium with a solid solution having the composition $x = 0.5$, is used to show that the saturation curves intersect at a common point with a value of 1, demonstrating that equilibrium of the solid solution and stoichiometric solid coincide. In Fig. 1b, equilibrium is perturbed relative to the solution in Figure 1a by increasing the amount of component A by a small factor of 1.05. The stoichiometric solids with compositions x_a and x_b are both saturated, but solid compositions in the interval x_a to x_b are supersaturated and can precipitate. Outside this interval the solid would dissolve if present.

For a non-ideal solid solution, depending on the solid activity coefficients, and hence the excess free energy, the second derivative may be positive or negative and the issue of stability is more complex (Prigogine and Defay, 1969). In terms of the saturation state, simultaneous equilibrium of solid compositions x_m and x'_m imply the relations

$$S_i^m(x_m) = \frac{K_i^m Q_i^m}{a_i^m} = 1, \tag{2.25a}$$

and

$$S_i^m(x'_m) = \frac{K_i^m Q_i^m}{(a_i^m)'} = 1. \tag{2.25b}$$

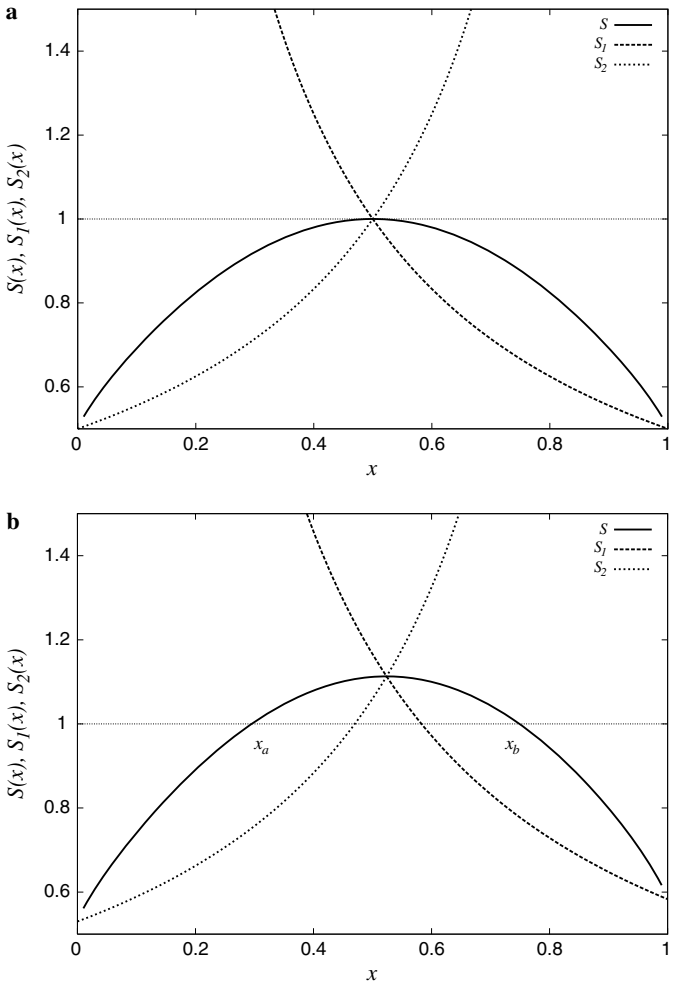

Fig. 1. Stoichiometric saturation state $S(x)$, and end member saturation states $S_1(x)$ and $S_2(x)$ for an ideal binary solid solution plotted as a function of composition x for: (a) stable equilibrium of a stoichiometric solid with composition 0.5, and (b) unstable equilibrium of stoichiometric solids with compositions x_a and x_b.

Clearly, the stoichiometric saturation states are also unity: $S_{x_m}(x_m) = S_{x'_m}(x'_m) = 1$. Equating $S_i^m(x_m)$ and $S_i^m(x'_m)$ yields

$$\frac{K_i^m Q_i^m}{a_i^m} = \frac{K_i^m Q_i^m}{(a_i^m)'}, \tag{2.26}$$

or

$$a_i^m = (a_i^m)', \tag{2.27}$$

equivalent to equality of the chemical potentials [Eq. (2.19)]. Conversely, if the stoichiometric solids corresponding to compositions x_m and x'_m of the exsolved phases are in equilibrium, then the solid solution is in equilibrium for the two compositions provided that $\partial \ln S_{x_m}/\partial x_l^m|_{x_m,x'_m} = 0$ (i.e., the equilibrium points are common intersection points with the end members, and they represent stable equilibria).

Equilibrium states that satisfy Eq. (2.26) for a non-ideal solid solution may be stable or unstable. If, for a non-ideal binary solid solution, the second derivative is negative, then the same arguments given above for ideal solid solutions apply and the equilibrium state is stable. If the second derivative of the saturation is positive, then the state is unstable and the solid solution will exsolve, if kinetically possible, into stable solid compositions determined by the miscibility gap in the free energy. In the presence of a miscibility gap, two maxima may occur in the stoichiometric saturation curve separated by a minimum. The maxima correspond to the most stable compositions on either side of the solvus. This is demonstrated in Fig. 2a which is calculated for the unique solution composition in equilibrium with compositions on both sides of the solvus (see Section 3.1.2 below for parameters used to generate the figures). The saturation curves for the stoichiometric solid [Eq. (2.16)] and end members [Eq. (2.18)] all intersect at a common value of 1 at the points x and x'. The first derivatives at points x, x', and x'' are all zero, but points x and x' have a negative second derivative (and are thus stable), whereas point x'' has a positive second derivative (and is thus unstable).

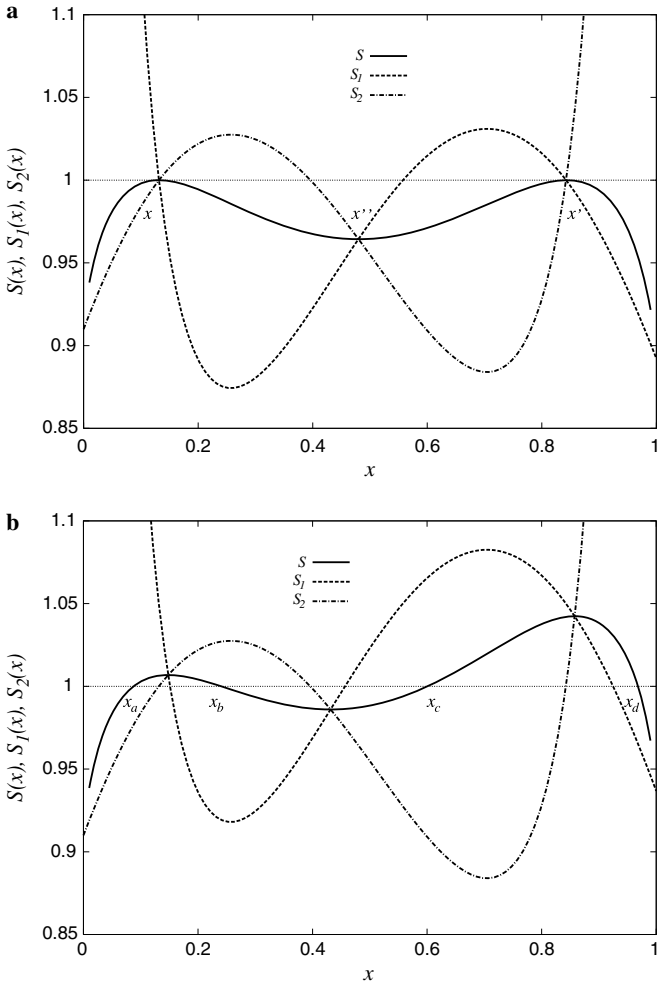

Fig. 2. Stoichiometric saturation state $S(x)$, and end member saturation states $S_1(x)$ and $S_2(x)$ for a non-ideal binary solid solution plotted as a function of composition x for: (a) stable equilibrium at compositions x and x', and (b) unstable equilibrium of stoichiometric solids with compositions x_a, x_b, x_c, and x_d.

If the aqueous solution is perturbed away from equilibrium by increasing the concentration of component A by a factor of 1.05, local equilibria occur, but as shown in Fig. 2b they are unstable (points labeled x_a, x_b, x_c, and x_d). As a consequence, stoichiometric solid compositions in the intervals x_a–x_b and x_c–x_d are both supersaturated and precipitate, and compositions outside these intervals are undersaturated and dissolve.

2.3. Discrete solid solution formulation

Solid solutions are incorporated into mass conservation equations describing reactive transport in a porous medium by discretizing the solid solution composition into a sequence of stoichiometric solids with compositions labeled $x_{mk} = \{x^m_{1k_1}, \ldots, x^m_{N_m k_{Z_m}}\}$, where the subscripts $k_1, \ldots, k_{Z_m}$ refer to a particular discretization with Z_m different stoichiometric solids. This sequence of solid solutions forms a basis set with which to represent the continuous variation in composition of the actual solid solution. Discretizing each independent composition variable x^m_i into Z^m_i increments $\Delta x^m_{ik_n} = x^m_{ik_n} - x^m_{ik_{n-1}}$, gives a total of

$$Z_m = \prod_{i=1}^{N_m} Z^m_i, \tag{2.28}$$

different stoichiometric solid solutions. It should be noted that the choice of discretization can be quite flexible; presumably even adaptive meshing could be implemented that changes with time to reduce the number of compositions needed. Although not pursued further here, an adaptive solid solution mesh would appear to be the most efficient characterization.

As an example, consider the binary solid solution composed of end members AC and BC: $(\mathrm{AC})_x(\mathrm{BC})_{1-x} = \mathrm{A}_x\mathrm{B}_{1-x}\mathrm{C}$. A sequence of solid solutions is generated with compositions $\mathrm{A}_{x_k}\mathrm{B}_{1-x_k}\mathrm{C}$, for $x_k = x_{k_1}, \ldots, x_{k_Z}$. For example, $x_k = k/(Z-1)$, $(k = 0, \ldots, Z-1)$, for equal spacing which includes end members. Taking $Z = 101$, gives the sequence: $\{\mathrm{BC}, \mathrm{A}_{0.01}\mathrm{B}_{0.99}\mathrm{C}, \mathrm{A}_{0.02}\mathrm{B}_{0.98}\mathrm{C}, \ldots, \mathrm{A}_{0.99}\mathrm{B}_{0.01}\mathrm{C}, \mathrm{AC}\}$, resulting in the set of reactions

$$x_k\mathrm{A}^+ + (1-x_k)\mathrm{B}^+ + \mathrm{C}^- \rightleftharpoons \mathrm{A}_{x_k}\mathrm{B}_{1-x_k}\mathrm{C}. \tag{2.29}$$

A more complicated example is given by the ternary solid solution plagioclase: $\mathrm{An}_x\mathrm{Or}_y\mathrm{Ab}_{1-x-y} = \mathrm{Ca}_x\mathrm{K}_y\mathrm{Na}_{1-x-y}\mathrm{Al}_{1+x}\mathrm{Si}_{3-x}\mathrm{O}_8$, with end members $\mathrm{An} = \mathrm{CaAl_2Si_2O_8}$, $\mathrm{Or} = \mathrm{KAlSi_3O_8}$, and $\mathrm{Ab} = \mathrm{NaAlSi_3O_8}$. In this case, composition space has two degrees of freedom with the constraint: $0 \leqslant x + y \leqslant 1$. The end-member reactions have the form

$$\mathrm{Ca}^{2+} + 2\mathrm{Al}^{3+} + 2\mathrm{SiO}_{2(\mathrm{aq})} - 8\mathrm{H}^+ + 4\mathrm{H_2O} \rightleftharpoons \mathrm{Anorthite}, \tag{2.30a}$$

$$\mathrm{K}^+ + \mathrm{Al}^{3+} + 3\mathrm{SiO}_{2(\mathrm{aq})} - 4\mathrm{H}^+ + 2\mathrm{H_2O} \rightleftharpoons \mathrm{Orthoclase}, \tag{2.30b}$$

$$\mathrm{Na}^+ + \mathrm{Al}^{3+} + 3\mathrm{SiO}_{2(\mathrm{aq})} - 4\mathrm{H}^+ + 2\mathrm{H_2O} \rightleftharpoons \mathrm{Albite}, \tag{2.30c}$$

and the reaction for the stoichiometric solid solution $\mathrm{An}_x\mathrm{Or}_y\mathrm{Ab}_{1-x-y}$ is given by

$$\begin{aligned} &x\mathrm{Ca}^{2+} + y\mathrm{K}^+ + (1-x-y)\mathrm{Na}^+ + (1+x)\mathrm{Al}^{3+} \\ &\quad + (3-x)\mathrm{SiO}_{2(\mathrm{aq})} - 4(1+x)\mathrm{H}^+ \\ &\quad + 2(1+x)\mathrm{H_2O} \rightleftharpoons \mathrm{An}_x\mathrm{Or}_y\mathrm{Ab}_{1-x-y}. \end{aligned} \tag{2.31}$$

The stoichiometric coefficients appearing in this reaction correspond to the coefficients $\widetilde{\nu}_{jm}$ defined in Eq. (2.10). In the general case of N_m end members, the discretized composition must satisfy

$$0 \leqslant \sum_{i=1}^{N_m - 1} x^m_{ik} \leqslant 1. \tag{2.32}$$

2.3.1. Convergence weight factor

A requirement of the discrete solid solution formulation is that the solution to the reactive transport equations should converge to a unique result with refinement of the solid solution discretization. To understand the implications of this requirement, first note that the solid solution volume fraction φ_{x_m} is equal to the sum of the volume fractions of the individual stoichiometric solids $\varphi_{x_{mk}}$ according to

$$\varphi_{x_m} = \sum_{k=1}^{Z} \varphi_{x_{mk}}. \tag{2.33}$$

As discussed below this sum may or may not include the primary phase. Differentiating this expression with respect to time t gives

$$\frac{\partial \varphi_{x_m}}{\partial t} = \sum_{k=1}^{Z} \frac{\partial \varphi_{x_{mk}}}{\partial t}. \tag{2.34}$$

If the stoichiometric solids are treated as pure phases that are not associated with a solid solution, then one has the usual mass transfer equation

$$\frac{\partial \varphi_{x_{mk}}}{\partial t} = \overline{V}_{x_{mk}} I_{x_{mk}}, \tag{2.35}$$

where $\overline{V}_{x_{mk}}$ denotes the molar volume and $I_{x_{mk}}$ the reaction rate of the solid. Substituting this relation into Eq. (2.34) then gives

$$\frac{\partial \varphi_{x_m}}{\partial t} = \sum_{k=1}^{Z} \overline{V}_{x_{mk}} I_{x_{mk}}. \tag{2.36}$$

For the hypothetical situation that all rates are equal $(I_{x_{mk_1}} = I_{x_{mk_2}} = \cdots = I_{x_{mk_Z}})$, then this equation reduces to the expression

$$\frac{\partial \varphi_{x_m}}{\partial t} = Z\overline{V}_{x_{mk_1}} I_{x_{mk_1}}, \tag{2.37}$$

assuming equal molar volumes. This result is clearly incorrect: the total reaction rate should not be proportional to the number of solids included in the discretization. For convergence to be obtained the total rate must be independent of the discretization.

To remedy this situation, a weight factor $\omega_{x_{mk}} \leqslant 1$ is introduced with the property that

$$\sum_{k=1}^{Z} \omega_{x_{mk}} = 1. \tag{2.38}$$

The mass transfer equation for $\varphi_{x_{mk}}$ is replaced by the weighted rate

$$\frac{\partial \varphi_{x_{mk}}}{\partial t} = \overline{V}_{x_{mk}} \omega_{x_{mk}} I_{x_{mk}}. \tag{2.39}$$

Now if all rates are equal, one gets

$$\begin{aligned} \frac{\partial \varphi_{x_m}}{\partial t} &= \sum_{k=1}^{Z} \overline{V}_{x_{mk}} \omega_{x_{mk}} I_{x_{mk}} = \overline{V}_{x_{mk_1}} I_{x_{mk_1}} \sum_{k=1}^{Z} \omega_{x_{mk}} \\ &= \overline{V}_{x_{mk_1}} I_{x_{mk_1}}, \end{aligned} \tag{2.40}$$

which yields an overall rate for the solid solution which is independent of Z, and thus converges with refinement of the solid solution discretization.

As a consequence, the reaction rate of the solid solution is related to the rates of the individual stoichiometric solids through the weighted mean

$$I_{x_m} = \frac{1}{\overline{V}_{x_m}} \sum_{k=1}^{Z} \overline{V}_{x_{mk}} \omega_{x_{mk}} I_{x_{mk}}. \tag{2.41}$$

Similarly, the contribution of each stoichiometric solid to the total rate of reaction for aqueous species must also be weighted by the factor $\omega_{x_{mk}}$.

The difficulty now arises as to how to choose the weight factors ω_k. In the general case, not all rates will be equal and, furthermore, not all stoichiometric solids included in the discretization react at the same time within a given control volume. One approach is to construct ω_k inversely proportional to the number of reacting stoichiometric solids within any given control volume. Distinguishing between precipitation and dissolution, the number of reacting stoichiometric solids derived from a particular solid solution within a control volume is equal to

$$N_R^{\pm} = \sum_{k, I_{x_{mk}} \gtrless 0} 1 = \begin{cases} N_R^{+}, & I_{x_{mk}} > 0, \\ N_R^{-}, & I_{x_{mk}} < 0, \end{cases} \tag{2.42}$$

where N_R^{+} denotes the number of precipitating and N_R^{-} the number of dissolving stoichiometric solids. This yields the following ansatz for $\omega_{x_{mk}}$

$$\omega_{x_{mk}} = \frac{1}{N_R^{+}} \quad \text{if } I_{x_{mk}} > 0, \tag{2.43}$$

and

$$\omega_{x_{mk}} = \frac{1}{N_R^{-}} \quad \text{if } I_{x_{mk}} < 0. \tag{2.44}$$

For $I_{x_{mk}} = 0, \omega_{x_{mk}}$ is chosen equal to zero. Clearly Eq. (2.38) holds. Other choices for $\omega_{x_{mk}}$ are also possible. Since no general derivation of the form of $\omega_{x_{mk}}$ seems to be available, it is necessary ultimately to test this ansatz against experimental observation.

2.3.2. Interpretation of solid solution results

Two different interpretations of coexisting stoichiometric solid solution compositions are possible. One interpretation is to consider all stoichiometric solids derived from a particular solid solution as representing a single phase. The volume fraction of this phase is determined from Eq. (2.33), and its composition is obtained by averaging over the individual stoichiometric solids using a relation of the form

$$\langle x_i^m \rangle = \frac{1}{\varphi_{x_m}} \sum_k x_{ik}^m \varphi_{x_{mk}}, \tag{2.45}$$

where all quantities are referred to a single control volume. This interpretation is consistent with a view of the solid solution homogeneously changing composition with changing fluid conditions. An alternative interpretation is to distinguish between the initial primary phase and the precipitated secondary stoichiometric solids which are taken to form a separate phase. The definition of the weight factor $\omega_{x_{mk}}$ depends on the interpretation in terms of which solids are included in the sums in Eqs. (2.33) and (2.45).

The approach proposed here may be contrasted with the recent approach developed by Nourtier-Mazauric et al. (2005) for ideal solid solutions. In their approach, a single stoichiometric solid is allowed to precipitate corresponding to the least soluble phase or, equivalently, the phase with the greatest saturation state. After each time step, the solid solution composition and volume fraction are revised by mixing the precipitated phase in each control volume with the existing solid solution over a time step. In this way, a single phase is maintained with varying composition and amount. The updated solid solution is allowed to dissolve independently through a separate rate law from precipitation.

There are several differences with the approach taken by Nourtier-Mazauric et al. (2005) and the approach presented here. In this approach, all supersaturated compositions may precipitate (depending on the rate law used), and not just the least soluble composition allowing the kinetic formulation to provide a flexible means of determining the composition of the precipitated solid. The initial solid solution is treated as a stoichiometric pure phase which can continue to react until it disappears completely. During this process it is replaced by a number of secondary stoichiometric solids. As noted above, maintaining a distinction between primary and secondary phases of the same solid solution provides a means of modeling different dissolution/precipitation scenarios. The method is applicable to both ideal and non-ideal solid solutions, including the occurrence of miscibility gaps. An assumption of instantaneous mixing is not used which would appear difficult to generalize to non-ideal solid solutions in the presence of a miscibility gap where solids with distinct compositions may coexist as they exsolve from solution.

The Murphy and Smith (1988) approach is similar to the second alternative interpretation in that they maintained a

distinction between the primary phase which dissolves and precipitation of a porous surface layer. They were interested in the formation of a distinct secondary phase that can result in armoring of the primary phase through formation of a porous surface layer thereby reducing its surface area through some function of the amount of secondary precipitate. The Murphy and Smith approach only allows for irreversible precipitation of the most stable phase, simulating a Doerner–Hoskins process. The approach described here includes this as one end-member of a spectrum of precipitation processes that range from completely irreversible to reversible.

Other conceptual models can also be investigated through suitable manipulation of rate laws and surface areas. For example, irreversible precipitation (compositional zonation) can be described by imposing an irreversible rate law in which precipitated phases are not allowed to redissolve. Precipitation (dissolution) of only the most (least) saturated phase can be modeled by suitable adjustment of the rate law and weighting factors.

In the following a discretized basis set is used to approximate a continuous variation in solid solution composition, first in a reaction path formulation for both closed and open systems, and then applied to more general open systems involving advective and diffusive transport.

2.4. Reaction path formulation

The discretized solid-solution formulation is implemented by first deriving equations for a reaction path in a closed or open system (Helgeson, 1968). For the purpose of this study, a system is closed if there is no mass transfer either into or out of the system (Prigogine and Defay, 1969). As a consequence, species concentrations can vary only as a result of physico-chemical processes taking place within the system. In an open system, mass transfer may take place with its surroundings. In a closed system, the final equilibrium state of the system is independent of the reaction path, and hence kinetics; whereas in an open system the final equilibrium state in general depends on the path (Prigogine and Defay, 1969).

A general geochemical system is considered allowing for both homogeneous reactions between aqueous species and heterogeneous solid solution reactions. Homogeneous reactions can be expressed in terms of a set of N_c primary or basis species $\mathcal{A}_j (j = 1, \ldots, N_c)$ with the form

$$\sum_j v_{ji}^{\mathrm{aq}} \mathcal{A}_j \rightleftharpoons \mathcal{A}_i, \tag{2.46}$$

for the aqueous secondary species $\mathcal{A}_i$ with stoichiometric coefficients v_{ji}^{aq} (Lichtner, 1985). Heterogeneous reactions between the aqueous fluid and solids have the form of Eq. (2.8) for each stoichiometric solid solution composition (pure phases have a single composition with a mole fraction of unity)

$$\sum_{ji} x_{ik}^m v_{ji}^m \mathcal{A}_j \rightleftharpoons \mathcal{M}_{x_{mk}}. \tag{2.47}$$

A reaction path is then described by the equations

$$\frac{\mathrm{d}}{\mathrm{d}t} \varphi \Psi_j(t) = -\sum_{mik} v_{ji}^m x_{ik}^m \omega_{x_{mk}} I_{x_{mk}}(t), \tag{2.48}$$

for the aqueous primary species, and

$$\frac{\mathrm{d}}{\mathrm{d}t} \varphi_{x_{mk}}(t) = \overline{V}_{x_{mk}} \omega_{x_{mk}} I_{x_{mk}}, \tag{2.49}$$

for the stoichiometric solid solution corresponding to the kth discretized composition, with weight factor $\omega_{x_{mk}}$ defined in Eq. (2.42). In these equations, φ denotes the aqueous volume fraction within the batch reactor, Ψ_j represents the total concentration accounting for aqueous secondary species given by

$$\Psi_j = \rho_f \left(m_j + \sum_i v_{ji}^{\mathrm{aq}} m_i \right), \tag{2.50}$$

where ρ_f refers to the fluid density, and m_j, m_i refer to the molality of the jth primary species and ith secondary species, respectively. Assuming conditions of local equilibrium, the secondary species concentrations are determined by the primary species concentrations through mass action equations of the form

$$m_i = \gamma_i^{-1} K_i^{\mathrm{aq}} \prod_j (\gamma_j m_j)^{v_{ji}^{\mathrm{aq}}}, \tag{2.51}$$

where $\gamma_{j,i}$ denote activity coefficients of the subscripted species, and K_i^{aq} denotes the equilibrium constant. The quantity $\varphi_{x_{mk}}$ denotes the solid solution volume fraction for the kth composition. The reaction rate $I_{x_{mk}}$ is assumed to have the usual form given by transition state theory

$$I_{x_{mk}} = -k_{x_{mk}} A_{x_{mk}} (1 - S_{x_{mk}}) \zeta_{x_{mk}}(\varphi_{x_{mk}}, S_{x_{mk}}) \mathcal{F}_{x_{mk}}(\varphi_{x_{mk}}^0), \tag{2.52}$$

where the rate constant $k_{x_{mk}}$ in general depends on the solid solution composition, and $A_{x_{mk}}$ denotes the specific solid surface area. The factors $\zeta_{x_{mk}}$ and $\mathcal{F}_{x_{mk}}$ restrict the rate in various cases. The quantity $\zeta_{x_{mk}}$ constrains the reaction rate to zero if the solid $\mathcal{M}_{x_{mk}}$ is undersaturated and not present in the system. It is defined as unity if $\varphi_{x_{mk}} > 0$ or $S_{x_{mk}} > 1$, and zero otherwise. The factor $\mathcal{F}_{x_{mk}}$ allows for irreversible reaction to take place in which secondary precipitates (defined as having zero initial concentration: $\varphi_{x_{mk}}^0 = 0$) are not allowed to back react and re-dissolve, and thus re-equilibrate with the fluid. In this case, precipitates that cannot dissolve simulate formation of layers (armoring). Thus the quantity $\mathcal{F}_{x_{mk}} = 1$ for reversible reaction for which complete re-equilibration of secondary solid products with the fluid takes place (Berthelot, 1872; Nernst, 1891). For irreversible reaction for which precipitated solids do not re-equilibrate with the fluid (Doerner and Hoskins, 1925), $\mathcal{F}_{x_{mk}} = 0$ if $\varphi_{x_{mk}}(t) > 0$ and $\varphi_{x_{mk}}^0 = 0$ and $S_{x_{mk}} < 1$; and $\mathcal{F}_{x_{mk}} = 1$ otherwise. Thus, dissolution of secondary solid solution compositions is prohibited.

The kinetic rate constant $k_{x_{mk}}$ is normalized to the surface area of the reacting solid. Experimental determination of surface area and the characterization of how it changes

both spatially and temporally with reaction is perhaps one of the most difficult aspects of quantitatively describing fluid/rock interactions. To complicate matters, there appears to be no reason why the surface area should be the same for precipitation and dissolution. The surface area for dissolution is proportional to the dissolving mineral grain size, with the actual reactive surface area determined by such factors as surface roughness and grain size distribution. The surface area for precipitation, on the other hand, is not necessarily limited by the precipitating phase itself and could be related to the total area of the porous medium. Alternatively, preferential nucleation could restrict the reaction to specific sites. Surface armoring is another process affecting surface area that is especially important in the case of solid solutions where it can prevent re-equilibration of the precipitated solid, resulting in the formation of isolated layers of differing composition. Finally, the change in surface area with reaction would generally be expected to behave differently for precipitation compared to dissolution, where in the latter case the surface area must vanish when the mineral completely dissolves.

To complete the reaction path equations represented by Eqs. (2.48) and (2.49), it also necessary to specify initial values for the fluid composition $\Psi_j(0) = \Psi_j^0$ and reacting solid $\varphi_{x_{mk}}(0) = \varphi^0_{x_{mk}}$. Various constraints can be applied to determine the initial fluid composition, such as pH and equilibrium with specified solids or gases. If the initial fluid is in equilibrium with respect to a specific solid solution composition, for example, this requires applying the appropriate mass action constraints for each end member.

Note that the composition variable x_m does not appear in the governing equations. With this formulation, the solid solution composition along the reaction path is determined directly through solving the reaction path equations. In general, at each instant in time there will be in fact several stoichiometric solid solutions present, either dissolving or precipitating. Eventually, however, as the system approaches equilibrium either a single unique composition or at most two compositions can survive, with all other compositions being undersaturated. Whether one or two compositions are present in the calculated final state depends on the solid solution discretization interval used in the calculation and how close the exact final composition is to the composition included in the discretization. At any instant in time the average solid solution composition $\langle x_i^m \rangle$ is obtained from Eq. (2.45). The calculated solid compositions in the final state should bracket the unique analytical solution for final solid solution composition (see below).

In a closed system, for which all stoichiometric compositions must be able to react, there exists a unique asymptotic equilibrium state independent of the reaction path (and hence the kinetic rate constants used to calculate the path) which is determined in the limit $t \to \infty$. Integrating the reaction path equations over time yields (taking $\varphi \simeq$ constant)

$$\int_0^\infty \frac{\mathrm{d}}{\mathrm{d}t}\varphi \Psi_j \,\mathrm{d}t = \varphi(\Psi_j^{\mathrm{eq}} - \Psi_j^0), = -\sum_{mik} \nu_{ji}^m x_{ik}^m \int_0^\infty \omega_{x_{mk}} I_{x_{mk}}(t)\,\mathrm{d}t, \tag{2.53}$$

and

$$\int_0^\infty \frac{\mathrm{d}}{\mathrm{d}t}\varphi_{x_{mk}}(t)\,\mathrm{d}t = \varphi^{\mathrm{eq}}_{x_{mk}} - \varphi^0_{x_{mk}}, = \overline{V}_{x_{mk}} \int_0^\infty \omega_{x_{mk}} I_{x_{mk}}\,\mathrm{d}t, \tag{2.54}$$

where Ψ_j^{eq}, $\varphi^{\mathrm{eq}}_{x_{mk}}$ refer to the final equilibrium state of the system as $t \to \infty$, and Ψ_j^0, $\varphi^0_{x_{mk}}$ refer to the initial state at $t = 0$. Eliminating the integral over the reaction rate gives the relation

$$\varphi(\Psi_j^{\mathrm{eq}} - \Psi_j^0) = -\sum_{mik} \nu_{ji}^m x_{ik}^m \overline{V}^{-1}_{x_{mk}} \omega_{x_{mk}} (\varphi^{\mathrm{eq}}_{x_{mk}} - \varphi^0_{x_{mk}}), \tag{2.55}$$

which, taking into account the initial solid solution composition and the survival of a single composition in the final equilibrium state, becomes

$$\varphi(\Psi_j^{\mathrm{eq}} - \Psi_j^0) = -\sum_{mi} \nu_{ji}^m \big(x^m_{ik_{\mathrm{f}}} \overline{V}^{-1}_{x_{mk_{\mathrm{f}}}} \omega_{x_{mk_{\mathrm{f}}}} \varphi^{\mathrm{eq}}_{x_{mk_{\mathrm{f}}}} - x^m_{ik_0} \overline{V}^{-1}_{x_{mk_0}} \omega_{x_{mk_0}} \varphi^0_{x_{mk_0}}\big), \tag{2.56}$$

where k_0 denotes the initial solid solution composition present at $t = 0$, and k_{f} denotes the final solid solution composition as $t \to \infty$. Because only one stoichiometric solid is presumed present in the initial and final states, $\omega_{x_{mk_{\mathrm{f}}}} = \omega_{x_{mk_0}} = 1$. This relation combined with the mass action equations for each end member of the final state solid solution enables the final equilibrium state to be calculated directly, including the final composition of the solid solution and its concentration. Note that there are an equal number of unknowns as equations: $N_c + \sum N_m$, for the N_c primary species concentrations, and for each solid solution included in the system a single volume fraction and $N_m - 1$ composition variables. Because the equations are nonlinear, an iterative approach (e.g., Newton–Raphson) is generally required to solve the system of equations (Glynn et al., 1990). By solving the reaction path equations the final composition is determined as part of the solution within the solid solution discretization error used in the calculation. Depending on how close the discretized solids are to the exact result, either one or at most two solid compositions which bracket the exact composition, can be present in the final reaction path equilibrium state. For the case of an open system in which irreversible reaction takes place, it is necessary to solve the reaction path equations numerically to obtain the final equilibrium state. In this case, the final state depends on the path and hence the kinetic rate constants used in the path calculation.

Depending on the relative rate constants, initial solid composition and abundance, and the initial aqueous concentrations, different reaction paths result. However, be-

cause the reaction path equations are linear in the kinetic rate constants, scaling the rate constants by a common factor σ simply results in scaling the time by the reciprocal factor σ^{-1} according to the following relations (Lichtner, 1993)

$$\Psi_j(\sigma t|k) = \Psi_j(t|\sigma k), \tag{2.57a}$$

$$\varphi_{x_{mk}}(\sigma t|k) = \varphi_{x_{mk}}(t|\sigma k), \tag{2.57b}$$

for some constant scale factor σ. As a consequence, if all rate constants are scaled by the same factor, preserving relative rates, the reaction path becomes stretched or compressed in time. Thus the time to reach equilibrium decreases or increases depending on whether σ is greater or less than one, respectively. This observation holds for both closed and open systems. However, for a closed system, because the final equilibrium state is independent of the path, changing the rate constants in some arbitrary manner only affects the path but not the final equilibrium state. If the reaction path is projected onto a Lippmann diagram (see below and Appendix B), time is eliminated, and the path is invariant with respect to scaling the kinetic rate constants.

2.5. Reactive transport equations

For an open system involving advection, dispersion, and diffusion the incorporation of solid solution reactions becomes more complex because the solid solution composition may vary spatially as well as temporally. The mass conservation equations for reaction of a discretized set of stoichiometric solid solutions involving advective and diffusive transport in a porous medium with porosity φ can be written in the following form for aqueous primary species as

$$\frac{\partial}{\partial t}\varphi\Psi_j + \nabla\cdot\boldsymbol{\Omega}_j = -\sum_{mik} \nu_{ji}^m x_{ik}^m \omega_{x_{mk}} I_{x_{mk}}, \tag{2.58}$$

and for stoichiometric solid solutions as

$$\frac{\partial}{\partial t}\varphi_{x_{mk}} = \overline{V}_{x_{mk}}\omega_{x_{mk}} I_{x_{mk}}, \tag{2.59}$$

with Ψ_j given by Eq. (2.56), and where $\varphi_{x_{mk}}$ denotes the volume fraction of the stoichiometric solid solution with the indicated composition. The total primary species flux Ω_j for species-independent diffusion is given by (Lichtner, 1985)

$$\boldsymbol{\Omega}_j = [-\tau\varphi D\nabla + \mathbf{q}]\Psi_j, \tag{2.60}$$

where τ denotes the tortuosity, D the diffusion/dispersion coefficient, and $\mathbf{q}$ the Darcy flow velocity. The reaction rate $I_{x_{mk}}$ has the same form given in Eq. (2.52) as used in the reaction path formulation. As in the reaction path case each stoichiometric solid solution can react either reversibly or irreversibly and secondary precipitates may or may not be allowed to redissolve and thus re-equilibrate with the fluid.

The result of reactive transport calculations with pure mineral phases is a sequence of reaction zones containing different mineral assemblages (Lichtner et al., 1996). Solving the transport equations directly determines the reacting mineral assemblages. For the case with solid solutions, a similar picture emerges but in this case a solid solution reaction zone, in general, consists of a homogeneous phase with a continuously spatially variable composition. In the discrete solid solution approach, the continuously variable composition expected of an actual solid solution is replaced with a coexisting set of compositions. The average solid solution composition within an alteration zone can be determined from Eq. (2.45) applied to each spatial node n.

Scaling relations also apply to the advection, dispersion, diffusion equation, similar to that for the reaction path equation with some additional complications resulting from dispersion and diffusion (Lichtner, 1993). One has

$$\Psi_j(\sigma\mathbf{r}, \sigma t|\mathbf{q}, D, k) = \Psi_j(\mathbf{r}, t|\mathbf{q}, \sigma^{-1}D, \sigma k), \tag{2.61a}$$

$$\varphi_{x_{mk}}(\sigma\mathbf{r}, \sigma t|\mathbf{q}, D, k) = \varphi_{x_{mk}}(\mathbf{r}, t|\mathbf{q}, \sigma^{-1}D, \sigma k), \tag{2.61b}$$

in which both the dispersion/diffusion coefficient and rate constants are scaled simultaneously.

2.5.1. Local chemical equilibrium

The kinetic formulation of reaction rates should reduce to the local equilibrium limit as the rate constants are allowed to approach infinity (Lichtner, 1985). To demonstrate that the local equilibrium limit holds for the discrete-composition solid solution formulation, Eq. (2.59) is substituted into Eq. (2.58) to give after rearranging the transport equations

$$\frac{\partial}{\partial t}\left(\varphi\Psi_j + \sum_{mik} \nu_{ji}^m x_{ik}^m \overline{V}_{x_{mk}}^{-1}\varphi_{x_{mk}}\right) + \nabla\cdot\boldsymbol{\Omega}_j = 0. \tag{2.62}$$

In this equation, all reference to reaction rates has been eliminated. Combining the transport equations with the appropriate mass action equations given by Eq. (2.13) results in the local equilibrium limit. Solving the local equilibrium equations requires determining not only the solid abundance and composition, but also the region in space where it is stable. Details of implementing the local equilibrium limit for pure solid phases can be found in Lichtner (1990). For an ideal solid solution or in the absence of a miscibility gap for nonideal, within each control volume solutions the sum in Eq. (2.62) collapses to a single term (or at most two terms) corresponding to the stoichiometric solid in equilibrium with the aqueous solution. Reaction rates for the stoichiometric minerals can be computed from Eq. (2.59) once the solution has been obtained. Note that the weight factor $\omega_{x_{mk}}$ does not appear in the local equilibrium limiting equations.

In an exact formulation, N_m mass action equations given by Eq. (2.4) are required corresponding to each end member of the solid solution. The mass conservation equations combined with the end member mass action equations then determine both the amount and composition of the solid solution within each control volume, and the spatial region of stability.

3. Application to the binary solid solution $A_xB_{1-x}C$

In this section, the kinetic discretized composition approach to incorporating solid solutions in reaction path and reactive transport equations is applied to a binary solid solution with end-member components AC and BC

$$A^+ + C^- \rightleftharpoons AC, \tag{3.1a}$$

$$B^+ + C^- \rightleftharpoons BC, \tag{3.1b}$$

in a three component system with aqueous species A^+, B^+, and C^-. The corresponding mass action equations are given by (cf. Section 2.1)

$$K_1 = \frac{a_1}{a_{A^+} a_{C^-}}, \tag{3.2a}$$

$$K_2 = \frac{a_2}{a_{B^+} a_{C^-}}, \tag{3.2b}$$

with aqueous activities a_{A^+}, a_{B^+}, and a_{C^-}, and solid activities and equilibrium constants a_1, a_2, K_1, K_2, for end-member solids AC and BC, respectively. For an ideal solution solid

$$a_1 = x, \tag{3.3a}$$

$$a_2 = 1 - x, \tag{3.3b}$$

where x refers to the mole fraction of component AC. At equilibrium the solid and aqueous concentrations are related by the expression

$$\frac{a_{A^+}}{a_{B^+}} = \frac{K_2 \lambda_1(x) x}{K_1 \lambda_2(x)(1-x)}, \tag{3.4}$$

obtained from the ratio of Eqs. (3.2a) and (3.2b), with solid activity coefficients λ_1 and λ_2, in general, functions of the solid solution composition. Conversely for an ideal solid solution

$$x = \frac{1}{1 + \frac{K_2 a_{B^+}}{K_1 a_{A^+}}}. \tag{3.5}$$

Combining reactions 3.1a and 3.1b, the overall reaction of the stoichiometric solid solution $A_xB_{1-x}C$ has the form

$$x A^+ + (1-x) B^+ + C^- \rightleftharpoons x AC + (1-x) BC \rightleftharpoons A_x B_{1-x} C. \tag{3.6}$$

Equilibrium of the stoichiometric solid $A_xB_{1-x}C$ is determined from the relation

$$\left(\frac{K_1}{\lambda_1(x) x}\right)^x \left(\frac{K_2}{\lambda_2(x)(1-x)}\right)^{1-x} a_{A^+}^x a_{B^+}^{1-x} a_{C^-} = 1. \tag{3.7}$$

Defining the equilibrium constant for the stoichiometric solid solution as

$$K_{ss}(x) = \left(\frac{K_1}{\lambda_1(x) x}\right)^x \left(\frac{K_2}{\lambda_2(x)(1-x)}\right)^{1-x}, \tag{3.8}$$

the equilibrium condition can be expressed in terms of the saturation index S_{ss} defined as

$$S_{ss}(x) = K_{ss}(x) Q_{ss}(x) = 1, \tag{3.9}$$

where the ion activity product $Q_{ss}(x)$ is defined as

$$Q_{ss}(x) = a_{A^+}^x a_{B^+}^{1-x} a_{C^-}. \tag{3.10}$$

As noted above equilibrium of the stoichiometric solid $A_xB_{1-x}C$ does not imply equilibrium of the solid solution with composition x. This condition is only a necessary one, but not sufficient. In addition, equilibrium with either end member AC or BC must also be imposed on the system to obtain equilibrium with the solid solution.

An analytical solution can be derived for equilibrium with a given binary solid solution composition under ideal conditions and assuming unit activity coefficients. There are three unknowns m_{A^+}, m_{B^+}, and m_{C^-}, and three equations consisting of the mass action equations for AC and BC, and charge conservation. It follows that:

$$m_{A^+}(x) = \sqrt{\frac{x\lambda_1(x) K_1^{-1}}{1 + \frac{(1-x)\lambda_2(x) K_1}{x\lambda_1(x) K_2}}}, \tag{3.11a}$$

$$m_{B^+}(x) = \frac{(1-x)\lambda_2(x) K_1}{x\lambda_1(x) K_2} \sqrt{\frac{x\lambda_1(x) K_1^{-1}}{1 + \frac{(1-x)\lambda_2(x) K_1}{x\lambda_1(x) K_2}}}, \tag{3.11b}$$

$$m_{C^-}(x) = m_{A^+}(x) + m_{B^+}(x). \tag{3.11c}$$

An alternative approach to determining equilibrium conditions is based on a Lippmann diagram (Lippmann, 1980; Glynn et al., 1990). At equilibrium the following condition must hold (a general formulation for a multicomponent system is presented in Appendix B).

$$m_{C^-}(m_{A^+} + m_{B^+}) = \frac{a_1}{K_1} + \frac{a_2}{K_2}, \tag{3.12}$$

as follows from the mass action equations, Eqs. (3.2a) and (3.2b). It also follows that:

$$m_{C^-}(m_{A^+} + m_{B^+}) = \frac{1}{\frac{K_1}{\lambda_1} X_{A^+} + \frac{K_2}{\lambda_2} X_{B^+}}, \tag{3.13}$$

obtained by eliminating x from the mass action equations, where $X_{A,B}$ refers to the aqueous activity fractions

$$X_{A^+,B^+} = \frac{m_{A^+,B^+}}{m_{A^+} + m_{B^+}}. \tag{3.14}$$

Following Lippmann (1980), for a binary solid solution the solidus is defined as

$$\mathcal{L}(x) = \log\left[\frac{x\lambda_1}{K_1} + \frac{(1-x)\lambda_2}{K_2}\right], \tag{3.15}$$

and the solutus as

$$l(X_{A^+}) = -\log\left[\frac{K_1}{\lambda_1} X_{A^+} + \frac{K_2}{\lambda_2}(1 - X_{A^+})\right]. \tag{3.16}$$

Equilibrium is determined from the tie line determined by the equality

$$\mathcal{L}(x) = l(X_{A^+}), \tag{3.17}$$

where x and X_{A^+} are related through the equation

$$X_{A^+}(x) = \frac{xK_2\lambda_1(x)}{xK_2\lambda_1(x) + (1-x)K_1\lambda_2(x)}. \quad (3.18)$$

For non-ideal solid solutions, a Lippmann diagram for the solutus is constructed by solving Eq. (3.13) for X_{A^+} to give

$$X_{A^+}(x) = \frac{10^{-\mathcal{L}(x)} - K_2/\lambda_2(x)}{K_1/\lambda_1(x) - K_2/\lambda_2(x)}, \quad (3.19)$$

where $\mathcal{L}(x)$ refers to the solidus defined in Eq. (3.15).

3.1. Reaction path

In this section, the reaction path calculations in a closed system are presented to illustrate the discrete solid solution formulation. Although the discrete formulation only uses stoichiometric solids (which as already noted cannot uniquely define solid solution equilibria), the kinetic formulation together with incorporation of a range of stoichiometric solid compositions, enables the system to find the correct solid solution equilibrium state (within the accuracy of the discretization) as illustrated in the following reaction path simulations. A reaction path describing an aqueous solution reacting with a binary solid solution is defined through the kinetic mass transfer equations (neglecting changes in volume)

$$\varphi\rho_f \frac{dm_{A^+}}{dt} = -\sum_k x_k\omega_k I_{ss}(x_k), \quad (3.20a)$$

$$\varphi\rho_f \frac{dm_{B^+}}{dt} = -\sum_k (1-x_k)\omega_k I_{ss}(x_k), \quad (3.20b)$$

$$\varphi\rho_f \frac{dm_{C^-}}{dt} = -\sum_k \omega_k I_{ss}(x_k) = \frac{d}{dt}(m_{A^+} + m_{B^+}), \quad (3.20c)$$

for aqueous species with molalities m_{A^+}, m_{B^+}, and m_{C^-}, and fluid density ρ_f, and

$$\frac{\partial\varphi_{ss,k}}{\partial t} = \overline{V}_{ss}\omega_k I_{ss}(x_k), \quad (3.21)$$

for the solid phase with compositions $A_{x_k}B_{1-x_k}C$ with volume fraction $\varphi_{ss,k}$, where the reaction rate is given by the usual expression based on transition state theory

$$I_{ss}(x) = -k_{ss}(x)A_{ss}(\varphi_{ss})(1 - S_{ss}(x))\zeta\mathcal{F}, \quad (3.22)$$

where k_{ss} refers to the kinetic rate constant (in general a function of solid composition), A_{ss} denotes the specific surface area which depends on the solid composition through the mineral abundance, and the saturation index S_{ss} is defined by

$$S_{ss}(x) = \left(\frac{K_1}{x\lambda_1(x)}\right)^x \left(\frac{K_2}{(1-x)\lambda_2(x)}\right)^{1-x} a_{A^+}^x a_{B^+}^{1-x} a_{C^-}. \quad (3.23)$$

The quantities ζ and $\mathcal{F}$ are rate control factors to restrict dissolution to phases present in the system and for reversible and irreversible reaction, respectively (see Section 2.3). The sum over x_k is taken over a discretization of the solid solution composition which spans its composition space. The initial condition is specified by the aqueous composition $m^0_{A^+}$, $m^0_{B^+}$, $m^0_{C^-}$, and initial solid with abundance specified by φ^0_{ss,k_0} with composition x_{k_0}.

The set of reactive minerals consist of a range of compositions of stoichiometric solid solutions, but not their corresponding end-member components for the corresponding compositions. Because of the discrete nature of the solid reactions included in the calculation, true equilibrium generally is not precisely achieved: one end member with the composition of the stoichiometric equilibrium solid may be slightly supersaturated and the other undersaturated, depending on the values for the equilibrium constants.

3.1.1. Ideal binary solid solution

First, reaction path calculations are conducted using the computer code FLOTRAN (Lichtner, 2001) for an ideal binary solid solution illustrating application of the discrete kinetic solid solution model. Two different solid solutions characterized by different solubilities between the two end-members were considered; this resulted in four different cases corresponding to equilibrium constants $K_1^{-1} = 0.75$ and $K_2^{-1} = 0.5$ (cases 1 and 2), and $K_1^{-1} = 7.5$ and $K_2^{-1} = 0.05$ (cases 3 and 4). These values are combined with two different initial conditions corresponding to an undersaturated aqueous solution ($m^0_{A^+} = 10^{-3}, m^0_{B^+} = 10^{-8}$ [mol/L]—cases 1, 3), and supersaturated solution ($m^0_{A^+} = 2, m^0_{B^+} = 2$ [mol/L]—cases 2, 4) with $m^0_{C^-} = m^0_{A^+} + m^0_{B^+}$. The solid solution composition is discretized using a composition step size of 0.02, with equal molar volumes of 100 cm^3/mol. For cases 1 and 3 an initial solid is present with composition and volume fraction with the values $\varphi^0_{A_{0.5}B_{0.5}C} = 0.1$ corresponding to $x_0 = 0.5$.

For a closed system with reversible reaction, the final equilibrium state may be computed directly from the mass conservation equations [see Eq. (2.56)]

$$\varphi\rho_f m^f_{A^+} + x_f\overline{V}^{-1}_{x_f}\varphi^f_{x_f} = \varphi\rho_f m^0_{A^+} + x_0\overline{V}^{-1}_{x_0}\varphi^0_{x_0}, \quad (3.24a)$$

$$\varphi\rho_f m^f_{B^+} + (1-x_f)\overline{V}^{-1}_{x_f}\varphi^f_{x_f} = \varphi\rho_f m^0_{B^+} + (1-x_{x_0})\overline{V}^{-1}_{x_0}\varphi^0_{x_0}, \quad (3.24b)$$

$$\varphi\rho_f m^f_{C^-} + \overline{V}^{-1}_{x_f}\varphi^f_{x_f} = \varphi\rho_f m^0_{C^-} + \overline{V}^{-1}_{x_0}\varphi^0_{x_0}, \quad (3.24c)$$

together with the mass action equations

$$K_1 m^f_{A^+} m^f_{C^-} = x_f, \quad (3.25a)$$

$$K_2 m^f_{B^+} m^f_{C^-} = 1 - x_f. \quad (3.25b)$$

In these equations, the superscript 0 denotes the initial state, and x_0 refers to the initial solid solution composition. The superscript 'f' refers to the final equilibrium state with solid solution composition x_f. There are five unknowns consisting of $m^f_{A^+}$, $m^f_{B^+}$, $m^f_{C^-}$, $\varphi^f_{x_f}$, and the final solid solution composition x_f, and an equal number of equations. The composition variable x_f can be eliminated by taking the ratio of the mass action equations to give

$$x_f = \frac{K_1 m^f_{A^+}}{K_1 m^f_{A^+} + K_2 m^f_{B^+}}. \quad (3.26)$$

Furthermore, it follows from the reaction path equations that

$$m^{\mathrm{f}}_{\mathrm{C}^-} = m^{\mathrm{f}}_{\mathrm{A}^+} + m^{\mathrm{f}}_{\mathrm{B}^+}. \tag{3.27}$$

As a result, the system of equations is reduced to three equations in three unknowns.

Shown in Table 1 is a comparison of the exact solution with the reaction path calculation for the four different cases. As can be seen by inspecting the table, the reaction path results are close to the analytical solution. The volume fractions representing the integrated rate over time exhibit excellent agreement with the analytical solution. In cases 1 and 4, two solid compositions bracket the analytical result in the final equilibrium reaction path state. It should be kept in mind, however, that because the system is closed the final equilibrium state is independent of the path and therefore the agreement between the numerical path calculations and analytical solution cannot be used to justify the form of the weight factor used in the calculations.

Cases 1 and 3 are characterized by a steady change in solution composition as the initial solid dissolves stoichiometrically until the system solutus is reached (Figs. 3 and 5). As the solution intersects the solutus, the solid dissolves incongruently by precipitation of new compositions which are slightly supersaturated with respect to the aqueous solution. With further reaction, the original solid continues to decrease in abundance and both the liquid and newly precipitated solids evolve in composition. At each time step, several solids are present all with compositions near the average. Each of these solids first increase and then decrease in abundance, as the system evolves. The discontinuities in trend of the average solid composition and volume fractions reflect discretization (e.g., in Fig. 3 sharp bends in the curves correspond to the complete dissolution of one of the solids). The calculated kinetic dissolution path corresponds closely to an equilibrium path once the solutus is reached. The calculation predicts the coexistence of multiple product solids which are interpreted as representing the average composition of the new solid. In calculating the average composition, both the original solid and newly precipitated phases are included.

Cases 2 and 4 involve precipitation from an initially supersaturated solution (Figs. 4 and 6). In the calculation, the initial aqueous solution is supersaturated with respect to the entire solid solution, so that initially every solid composition precipitates. However, the kinetic formulation increases the rate of precipitation of solids that correspond to the solidus/solutus relations. As a consequence, precipitation enriches the aqueous solution in the soluble (B^+)

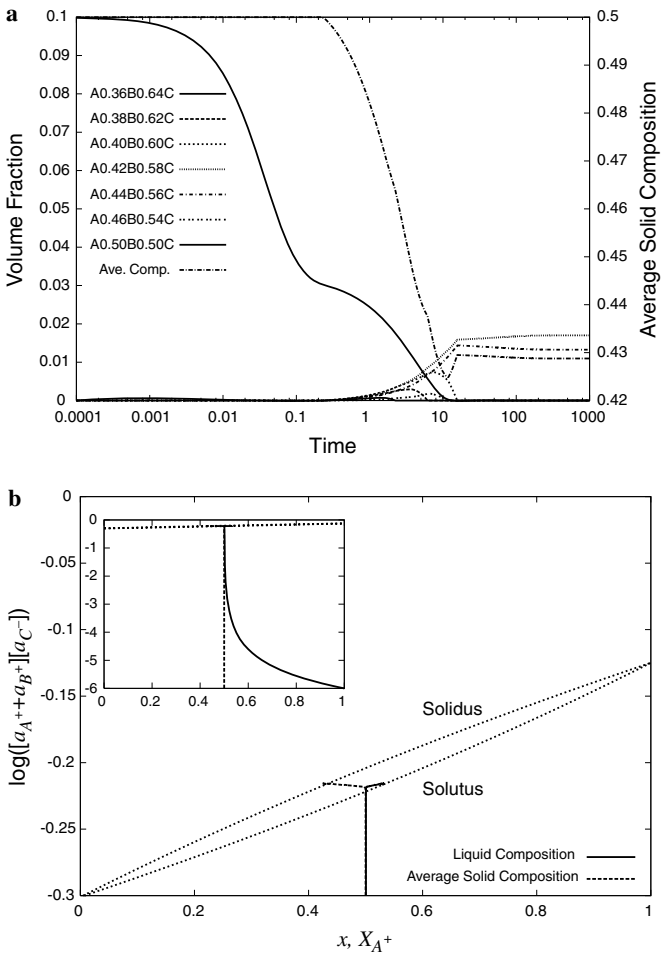

Fig. 3. Evolution of solids and aqueous solution resulting from dissolution of a stoichiometric solid solution with composition $A_{0.5}B_{0.5}C$ and with equilibrium constants $K_1 = 0.75$ and $K_2 = 0.5$ (case 1). (a) Solid volume fractions and average solid composition as a function of time; (b) the average solid and aqueous solution compositions plotted on a Lippmann diagram. The inset shows an expanded plot of the Lippmann variable.

Table 1
Comparison of the exact result with the final reaction path equilibrium state for four different cases (see text) involving reaction of an ideal binary solid solution using the kinetic, discrete-composition formulation

Case	m_{A^+}		m_{B^+}		m_{C^-}		x_f		φ_f	
	Exact	Path	Exact	Path	Exact	Path	Exact	Path	Exact	Path
1	0.4136	0.4138	0.3658	0.3657	0.7794	0.7795	0.4298	0.42	0.0299	0.0163
								0.44		0.0137
2	0.4574	0.4578	0.3301	0.3297	0.7874	0.7875	0.4802	0.48	0.3213	0.3231
3	0.5347	0.5367	0.0780	0.0778	0.6128	0.6145	0.0436	0.04	0.0449	0.0448
4	1.3499	1.3555	0.0273	0.0271	1.3772	1.3826	0.2479	0.24	0.2623	0.1798
								0.26		0.0820

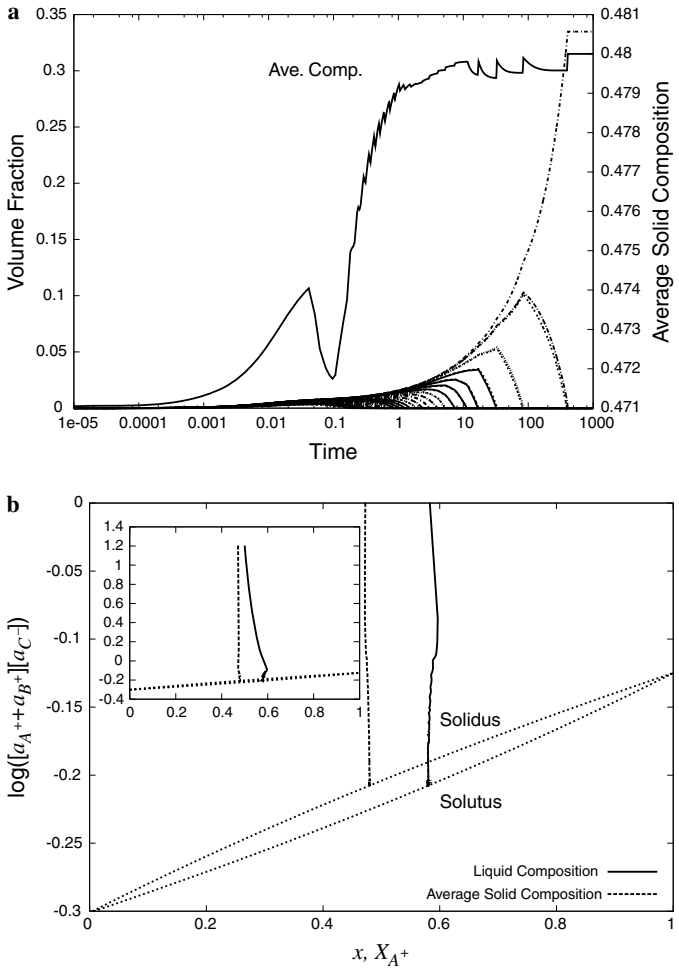

Fig. 4. Evolution of solids and aqueous solution during precipitation from a supersaturated solution with $K_1 = 0.75$ and $K_2 = 0.5$ (case 2). (a) Solid volume fractions and average solid composition as a function of time; (b) the average solid and the aqueous solution plotted on a Lippmann diagram. The insert shows an expanded plot of the Lippmann variable. In (a), all possible solids occur at the onset of reaction, although all but one gradually dissolve.

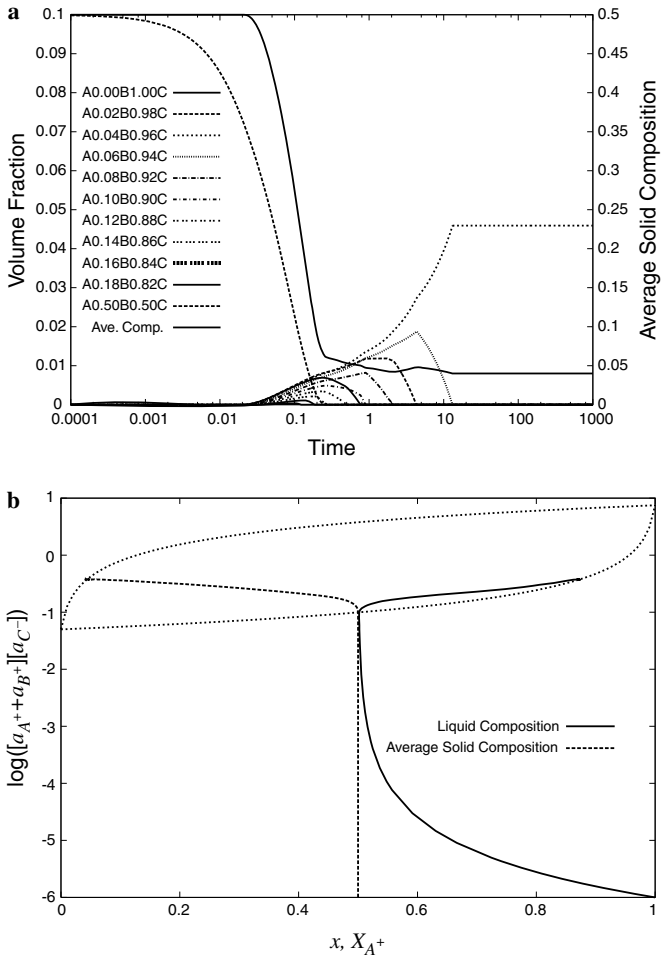

Fig. 5. Evolution of solids and aqueous solution resulting from dissolution of a stoichiometric solid solution with composition $A_{0.5}B_{0.5}C$ and with equilibrium constants $K_1 = 7.5$ and $K_2 = 0.05$ (case 3). (a) Solid volume fractions and average solid composition as a function of time; (b) the average solid and aqueous solution plotted on a Lippmann diagram.

component. As the system evolves, the aqueous solution and average solid composition approach steady compositions that are governed by the solidus/solutus relations. The movement of the aqueous solution back towards the insoluble component corresponds to the loss of the final competing solid (Figs. 4 and 6).

At equilibrium, either one or at most two solid compositions are present. Note that in Figs. 4a and 6a secondary precipitates occur in pairs although only a single phase survives as the system approaches equilibrium in Fig. 4a, whereas two survive in Fig. 6a.

The use of average compositions shows that the calculated system evolution is close to an equilibrium path. The small amount of supersaturation of the aqueous solution and solid compositions is a result of the use of kinetics to describe solid reactions. It is interesting to observe that although a large number of time steps are required before the system reduces to a single equilibrium solid, the average composition quickly approaches the final composition despite the presence of almost the complete suite of discrete compositions.

3.1.2. Nonideal binary solid solution

Next the method is applied to a nonideal binary solid solution. A two parameter Guggenheim (1952) model is used to represent the solid activity coefficients with the form

$$\ln \lambda_1(x) = (1-x)^2[\alpha_0 + \alpha_1(4x-1)], \tag{3.28a}$$

$$\ln \lambda_2(x) = x^2[\alpha_0 + \alpha_1(4x-3)], \tag{3.28b}$$

where the Guggenheim expansion coefficients have the values $\alpha_0 = 2.5$ and $\alpha_1 = -0.08$. Equilibrium constants with values $\log K_1 = 0.904$ and $\log K_2 = 1.129$ were used in the simulations. These values correspond to the KCl–KBr solid solution with the exception of the parameter α_0 which was increased from 1.2 to 2.5 to produce a miscibility gap.

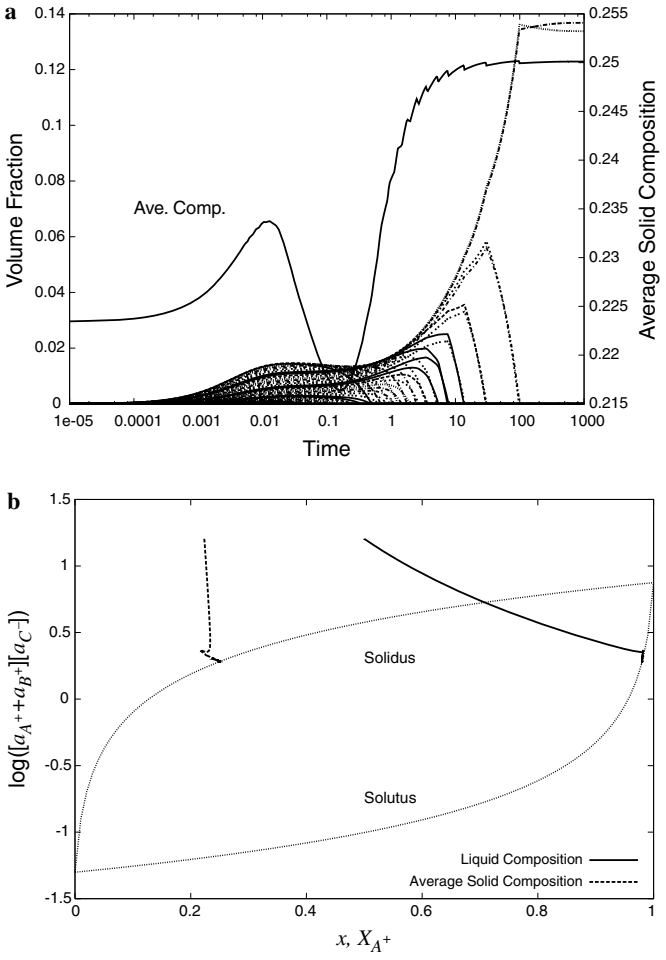

Fig. 6. Evolution of solids and aqueous solution during precipitation from an initially supersaturated solution with $K_1 = 7.5$ and $K_2 = 0.05$ (case 4). (a) Solid volume fractions and average solid composition as a function of time; (b) the average solid and aqueous solution plotted on a Lippmann diagram. In (a), all possible solids occur at the onset of reaction, although all but two gradually dissolve.

Three reaction path calculations were carried out with an initial aqueous solution undersaturated with respect to the solid solution ($m_{A^+} = 10^{-3}$ mol/L, $m_{B^+} = 10^{-8}$ mol/L, $m_{C^-} = m_{A^+} + m_{B^+}$). The first reaction path (#1) is calculated using equal effective kinetic rate constants for all solid compositions with the value 5×10^{-10} mol/cm^3/s, and with an initial solid composition and volume fraction equal to $\varphi^0_{A_{0.52}B_{0.48}C} = 0.1$. For the second path (#2) an initial solid composition and volume fraction equal to $\varphi^0_{A_{0.24}B_{0.76}C} = 0.9$ was used. In this case, different effective rate constants were used for the initial solid (10^{-8} mol/cm^3/s) and for secondary solids (10^{-10} mol/cm^3/s). In the third path (#3), the solid is the same as in path #2 but the initial solid volume fraction was reduced to 0.1. In all cases the initial phase is unstable and dissolves. For the first two reaction paths the system evolves to the same final equilibrium state shown on a Lippmann diagram in Fig. 7, consisting of two immiscible solids with compositions $\varphi_{A_{0.14}B_{0.86}C}$ and

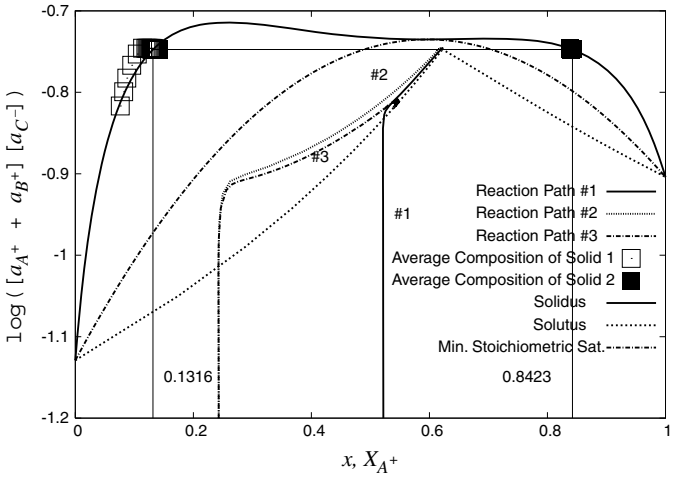

Fig. 7. Lippmann diagram and reaction path for an nonideal binary solid solution. Three reaction paths are illustrated (see text for details). For path #1 the initial solid has the composition $A_{0.52}B_{0.48}C$ with volume fraction $\varphi^0_{A_{0.52}B_{0.48}C} = 0.1$. The system comes to equilibrium with coexistence of the two phases $A_{0.14}B_{0.86}C$ and $A_{0.84}B_{0.16}C$. For path #2 an initial solid composition $A_{0.24}B_{0.76}C$ and volume fraction 0.9 is used. Path #3 corresponds to the same initial solid composition as path #2 but with a volume fraction of 0.1. Only the solids for path #1 are shown.

$\varphi_{A_{0.84}B_{0.16}C}$, but with different volume fractions. The second path, however, crosses the solutus and approaches the stoichiometric saturation curve. For the third path, because of the smaller initial volume fraction, two solids form with neighboring compositions $\varphi_{A_{0.06}B_{0.94}C}$ and $\varphi_{A_{0.08}B_{0.92}C}$. The solids are shown only for the first path. Note that there exists one unique fluid composition where two solid solution end members can coexist. However, whether or not the fluid can actually reach this composition depends on the total moles of each species available, determined by the initial fluid composition and abundance of the primary solid phase initially present.

These calculations also illustrate the flexibility of the discrete formulation to generate reaction paths. Path #1 in Fig. 7 shows a near equilibrium evolution of solid and liquid with precipitation occurring where the liquid crosses the solutus. Path #2 shows inhibited precipitation kinetics and allows the solution composition to move metastably above the solutus. By preventing any precipitation from occurring, the solid would dissolve along the minimum stoichiometric saturation line (not shown; cf. Glynn et al., 1990). By suitable manipulation of dissolution and precipitation rates and the factors governing reversible and irreversible behavior, a wide variety of reaction paths can be simulated.

The time evolution of the solid phase volume fractions for the first reaction path are shown in Fig. 8. As time increases the system comes to equilibrium with both solids on opposite sides of the miscibility gap. To understand this behavior the free energy of the mixture G_M/RT given by

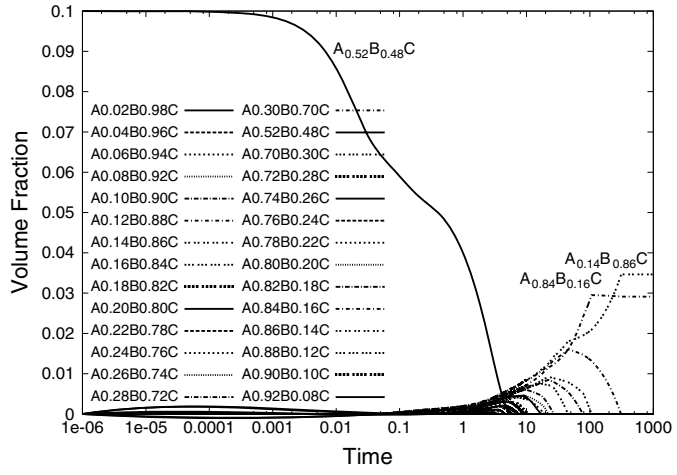

Fig. 8. Volume fractions for stoichiometric solids plotted as a function of time for the nonideal binary solid solution described in Fig. 7 for reaction path #1. The system comes to equilibrium with coexistence of the two phases $A_{0.14}B_{0.86}C$ and $A_{0.84}B_{0.16}C$.

$$\frac{G_M(x)}{RT} = \ln[(x\lambda_1(x))^x((1-x)\lambda_2(x))^{1-x}], \tag{3.29a}$$

$$= x(1-x)(\alpha_0+\alpha_1(2x-1)) + x\ln(x) + (1-x)\ln(1-x), \tag{3.29b}$$

is shown in Fig. 9 together with the relation between X_{A^+} and x given by Eq. (3.18). A miscibility gap occurs between $x = 0.132$ and $x = 0.842$; these are values obtained from the equality of the chemical potential in the two phases as demonstrated below. The final equilibrium state may be computed directly from the mass conservation equations [see Eq. (2.56)]. There are now seven unknowns, $\{m^f_{A^+}, m^f_{B^+}, m^f_{C^-}, \varphi^f_{x_f}, \varphi^f_{x'_f}, x_f, x'_f\}$, with an equal number of equations consisting of three mass conservation equations

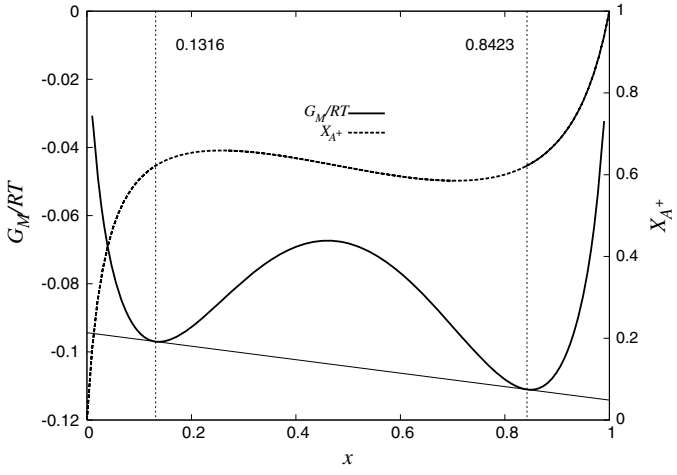

Fig. 9. Free energy G_M/RT and X_{A^+} plotted as a function of x for the nonideal binary solid solution used in Figs. 7 and 8. A miscibility gap obtained as the common tangent to the free energy curve appears between $x = 0.1316$ and $x = 0.8423$ as indicated in the figure by the vertical lines.

$$\varphi\rho_f m^f_{A^+} + x_f\overline{V}^{-1}_{x_f}\varphi^f_{x_f} + x'_f\overline{V}^{-1}_{x'_f}\varphi^f_{x'_f} = \varphi\rho_f m^0_{A^+} + x_0\overline{V}^{-1}_{x_0}\varphi^0_{x_0}, \tag{3.30a}$$

$$\varphi\rho_f m^f_{B^+} + (1-x_f)\overline{V}^{-1}_{x_f}\varphi^f_{x_f} + (1-x'_f)\overline{V}^{-1}_{x'_f}\varphi^f_{x'_f} = \varphi\rho_f m^0_{B^+} + (1-x_{x_0})\overline{V}^{-1}_{x_0}\varphi^0_{x_0}, \tag{3.30b}$$

$$\varphi\rho_f m^f_{C^-} + \overline{V}^{-1}_{x_f}\varphi^f_{x_f} + \overline{V}^{-1}_{x_f}\varphi^f_{x'_f} = \varphi\rho_f m^0_{C^-} + \overline{V}^{-1}_{x_0}\varphi^0_{x_0}, \tag{3.30c}$$

together with four mass action equations

$$K_1 m^f_{A^+} m^f_{C^-} = \lambda_1(x_f)x_f, \tag{3.31a}$$

$$K_2 m^f_{B^+} m^f_{C^-} = \lambda_2(x_f)(1-x_f), \tag{3.31b}$$

$$K_1 m^f_{A^+} m^f_{C^-} = \lambda_1(x'_f)x'_f, \tag{3.31c}$$

$$K_2 m^f_{B^+} m^f_{C^-} = \lambda_2(x'_f)(1-x'_f). \tag{3.31d}$$

Combining Eqs. (3.31a) and (3.31c), and Eqs. (3.31b) and (3.31d) provides two equations for the two compositions x_f and x'_f

$$x_f\lambda_1(x_f) = x'_f\lambda_1(x'_f), \tag{3.32a}$$

$$(1-x_f)\lambda_2(x_f) = (1-x'_f)\lambda_2(x'_f), \tag{3.32b}$$

equivalent to equality of the chemical potentials of the two phases: $\mu_1 = \mu'_1$, and $\mu_2 = \mu'_2$. The reaction path simulation is compared to the exact solution in Table 2. As can be seen, excellent agreement is obtained for the aqueous solution and solid composition, but as a result of numerical inaccuracies the solid phase volume fractions are only approximately correct. To improve the agreement a front tracking scheme would be needed to more closely follow the appearance and disappearance of solid phases.

3.2. Reactive transport with pure diffusion and advection-diffusion

An example simulation involving advection and diffusion in a one-dimensional column coupled to reaction of the solid solution $A_xB_{1-x}C$ is presented using the computer code FLOTRAN (Lichtner, 2001), to illustrate the discretized solid solution technique for an open system. The transport equations describing reaction with a solid solution in a porous medium with porosity φ are of the form

Table 2
Comparison of the exact result with the final equilibrium state of a reaction path calculation using the discretized solid solution formulation for a non-ideal binary solid solution

Quantity	Path #1		Path #2		Path #3	
	Exact	Path	Exact	Path	Exact	Path
m_{A^+}	0.2631	0.2631	0.2631	0.2631	0.2133	0.2099
m_{B^+}	0.1599	0.1599	0.1599	0.1599	0.1782	0.1796
m_{C^-}	0.4230	0.4230	0.4230	0.4230	0.3916	0.3894
x_f	0.1316	0.14	0.1316	0.14	0.0753	0.08
x'_f	0.8423	0.84	0.8423	0.84	—	—
φ_f	0.2202	0.2239	0.7614	0.7741	0.0648	0.0654
φ'_f	0.2587	0.2652	0.1344	0.1256	—	—

$$\frac{\partial \varphi C_{A^+}}{\partial t} + \nabla \cdot \mathbf{F}_{A^+} = -\sum_k x_k \omega_k I_{ss}(x_k), \tag{3.33a}$$

$$\frac{\partial \varphi C_{B^+}}{\partial t} + \nabla \cdot \mathbf{F}_{B^+} = -\sum_k (1 - x_k) \omega_k I_{ss}(x_k), \tag{3.33b}$$

$$\frac{\partial \varphi C_{C^-}}{\partial t} + \nabla \cdot \mathbf{F}_{C^-} = -\sum_k \omega_k I_{ss}(x_k), \tag{3.33c}$$

and

$$\frac{\partial \varphi_{ss,k}(\mathbf{r}, t)}{\partial t} = \overline{V}_{ss} \omega_k I_{ss}(x_k), \tag{3.34}$$

with fluxes

$$\mathbf{F}_j = \mathbf{q} C_j - \tau \varphi D \nabla C_j, \tag{3.35}$$

with Darcy velocity $\mathbf{q}$, tortuosity τ, and diffusion coefficient D.

Initial and boundary conditions must be specified to complete the set of equations. For initial or boundary conditions specifying equilibrium with a particular solid solution composition x_0, simultaneous equilibrium with respect to the solid solution end members corresponding to the desired composition must be determined. A porous medium with porosity 0.5 occupied by a solid solution with volume fraction 0.5 and composition $A_{0.5}B_{0.5}C$ is considered. Initially, the pore fluid in the column is in equilibrium with the solid solution. The injected fluid is taken to be in equilibrium with a solid solution with composition $A_{0.76}B_{0.24}C$. To describe the solid solution alteration, a discretization of 0.02 in composition is used from end member AC to BC.

The resulting mineral alteration pattern is shown in Fig. 10 for pure diffusive transport for a diffusion coefficient of 10^{-9} m^2/s and an effective rate constant of 10^{-8} mol/cm^3/s for all solids, corresponding to a time of 100 years. As can be seen from the figures, a sequence of secondary solid solutions is formed which vary spatially in composition, ranging from the initial composition ($A_{0.5}B_{0.5}C$), to the solid solution composition in equilibrium with the boundary fluid ($A_{0.76}B_{0.24}C$). The solid line represents the sum of the volume fractions of the alteration products. A relatively smooth envelope is obtained in spite of the sharply peaked profiles of the individual product solid solutions. The average composition derived from Eq. (2.45) is shown as a dash-dotted curve. The average composition evolves monotonically from $A_{0.76}B_{0.24}C$ to $A_{0.5}B_{0.5}C$ with small steps that reflect the discretization. The envelope of the summed volume fractions combined with the average composition data can be interpreted as representing a single homogeneous solid solution phase.

The effect of the solid solution discretization is shown in Figs. 11a and b for $Z = 50$, 100, and 200. Convergence of the total volume fraction for the secondary solid solution

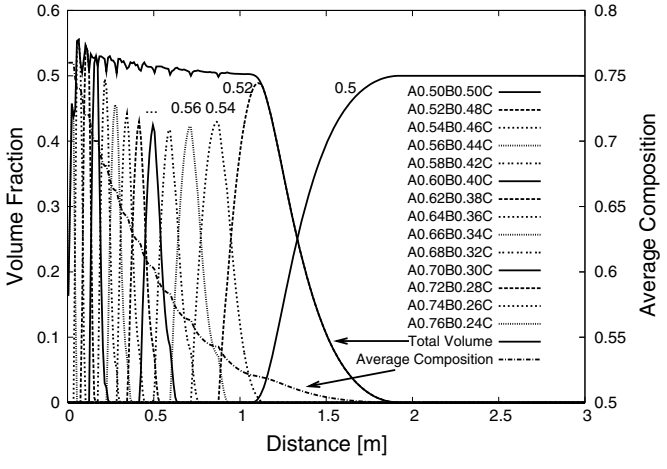

Fig. 10. Stoichiometric solid volume fractions plotted as a function of distance using $K_1^{-1} = 0.75$ and $K_2^{-1} = 0.5$ for an elapsed time of 100 years for pure diffusive transport and with an initial solid volume fraction and composition of $\varphi_{A_{0.5}B_{0.5}C} = 0.5$. Also shown is the summation of the secondary solid volume fractions representing the envelope of a separate secondary alteration phase and average solid composition. The labels $0.5, 0.52, 0.54, \ldots$, indicate the change in component A across the profile.

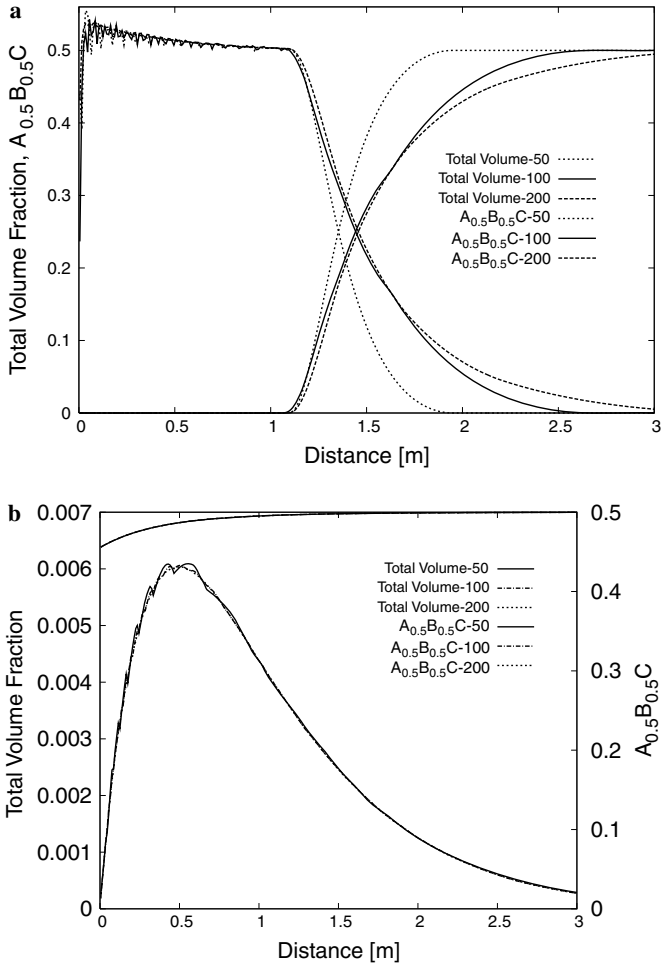

Fig. 11. Volume fractions for primary solid $A_{0.5}B_{0.5}C$ and total secondary solids for $Z = 50$, 100, and 200, plotted as a function of distance for pure diffusive transport with an elapsed time of 100 years. (a) The case shown in Fig. 10, with an effective rate constant of 10^{-8} mol/cm^3/s and, (b) an effective rate constant of 10^{-12} mol/cm^3/s. In (b) the primary solid profiles coincide.

is shown for two different rate constants corresponding to 10^{-8} mol/cm^3/s (Fig. 11a), and 10^{-12} mol/cm^3/s (Fig. 11b). For the larger rate constant, convergence improves significantly from $Z = 50$ to 100. The effects of discretization are more evident in the greater width of the reaction front for larger Z. Smaller rate constants yield smoother profiles and result in better convergence as evidenced in Fig. 11b. Greater discretization results in a smoother total volume envelope of the secondary precipitates.

The case of advective and diffusive transport is shown in Fig. 12 for a Darcy flow velocity of 1 m/y and a diffusion coefficient of 10^{-9} m^2/s. Note, however, the difference in spatial scales with a much larger alteration zone for the case with advective transport. A smooth envelope is obtained by summing the secondary products to yield the solid solution alteration phase.

3.2.1. Exchange reactions

Finally, it is noted that the discrete-composition formulation of solid solution reaction includes exchange reactions as a special case. Although, in general, the solid solution volume fraction changes with time and position, it is also possible that reaction is limited to exchange of species common to the solid solution without any change in volume fraction. For example, for the binary solid solution with end members AC and BC, the overall reaction

$$\mathrm{A^+ + BC \rightleftharpoons\ B^+ + AC}, \tag{3.36}$$

involves exchange of species A^+ and B^+. As a consequence species C^- is conserved. To see how this situation may arise from the reactive transport equations, Eqs. (3.33a)–(3.33c) are rewritten in terms of the transport operator $\mathcal{L} = \varphi\partial/\partial t + \mathbf{V}\cdot\mathbf{q} - \mathbf{V}\cdot\phi\tau D\mathbf{V}$ for simplicity, to give

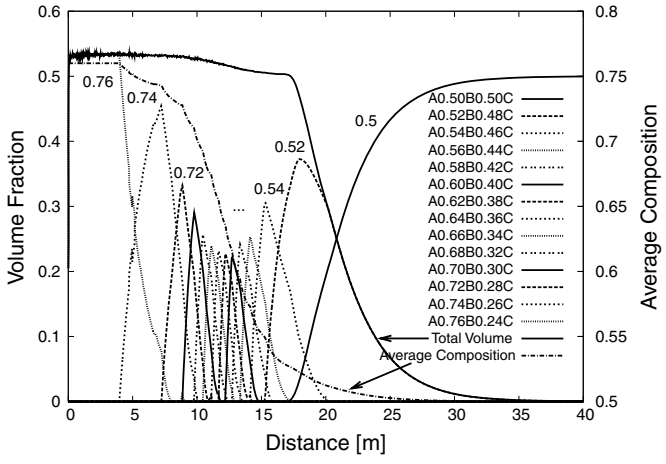

Fig. 12. Stoichiometric solid volume fractions plotted as a function of distance for $K_1^{-1} = 0.75$ and $K_2^{-1} = 0.5$ corresponding to an elapsed time of 100 years for advective and diffusive transport. An initial stoichiometric solid composition $A_{0.5}B_{0.5}C$ and volume fraction $\varphi_{A_{0.5}B_{0.5}C} = 0.5$ is used. Also shown is the summation of the secondary solid volume fractions representing the envelope of a separate secondary alteration phase and average solid composition. The labels $0.5, 0.52, 0.54, \ldots$, indicate the change in component A across the profile.

$$\mathcal{L}C_{A^+} = -\sum_k x_k\omega_k I_k = -I, \tag{3.37a}$$

$$\mathcal{L}C_{B^+} = -\sum_k (1-x_k)\omega_k I_k = I, \tag{3.37b}$$

$$\mathcal{L}C_{C^-} = -\sum_k \omega_k I_k = 0, \tag{3.37c}$$

and

$$\frac{\partial\varphi_k}{\partial t} = \overline{V}_k\omega_k I_k, \tag{3.38}$$

where the rate for species C^- is set to zero, and I is defined by

$$I = \sum_k x_k\omega_k I_k. \tag{3.39}$$

Note that species A^+ and B^+ involve equal and opposite rates. The total solid solution volume fraction then satisfies the equation (see Eq. (2.33))

$$\frac{\partial\varphi_{ss}(\mathbf{r},t)}{\partial t} = \frac{\partial}{\partial t}\sum_k \varphi_k(\mathbf{r},t) = \overline{V}_{ss}\sum_k \omega_k I_k = 0, \tag{3.40}$$

assuming the molar volume is independent of composition ($\overline{V}_k = \overline{V}_{ss}$), and thus the solid solution volume fraction is conserved.

Realization of a pure exchange process would not occur in most systems, but may be a good approximation in certain circumstances. For example, potassic alteration of feldspar at elevated temperatures involving exchange of Na^+ and K^+ can take place if aluminum is approximately conserved and silica is buffered by quartz. In the example presented above, if the species C^- occurs in sufficient concentrations compared to other species, it may be approximately conserved. In general, however, exchange reactions and precipitation and dissolution of a solid solution occur simultaneously.

4. Conclusion

This work demonstrates the feasibility of incorporating solid solutions in reactive transport models using a kinetic, discrete-composition formulation in which a discretized set of stoichiometric solid solution compositions are included in the set of reacting minerals with reaction rates governed by a kinetic rate law. A kinetic formulation of mineral reaction rates provides a convenient and straightforward means to implement solid solution reactions into mass conservation equations describing reactive transport in a porous media. The use of a kinetic formulation for solid reaction rates provides a self-determining mechanism for the solid solution composition. It was necessary, however, to introduce a weighting factor, applied separately for dissolution and precipitation reaction rates, to obtain convergence as the discretization of stoichiometric solids is refined. It was demonstrated that equilibrium of a stoichiometric solid is equivalent to equilibrium of the solid solution if and only if the stoichiometric solid is in a stable equilibrium state.

Unstable equilibrium compositions of the stoichiometric solid are ephemeral and eventually disappear with time—at these compositions the reaction rate merely changes sign. Because only stable equilibria can survive, the discrete stoichiometric approach must yield, within the accuracy of discretization, the same equilibria as the true solid solution. The method was applied to reaction paths in a closed system, and to open systems involving transport by advection, dispersion and diffusion. The latter resulted in formation of a spatially variable solid solution composition from alteration of an initial stoichiometric solid.

Acknowledgments

This material is based upon work supported by the National Science Foundation under Grant No. CHE-0431328 and the U.S. Department of Energy, Biological and Environmental Research (BER), LDRD-DR 20040042DR (Science of Geological Carbon Sequestration: Integration of Experimentation and Simulation), LDRD-DR 20030091DR (Actinide Partitioning at Solid-Solution Interfaces), and DOE-NETL Contract #05FE01. The authors thank Hari Viswanathan, Peter Alt-Epping, Pierre Glynn, and Richard Sack for their comments.

Associate editor: Dimitri A. Sverjensky

Appendix A. Stability analysis

In this appendix the stability of equilibrium of a stoichiometric solid solution with an aqueous solution is investigated. Differentiating the logarithm of the saturation S_{x_m} given in Eq. (2.15)

$$\ln S_{x_m} = \sum_{i=1}^{N_m} x_i^m \ln S_i^m, \tag{A.1}$$

with respect to x_l^m, $(l = 1, \ldots, N_m - 1)$, yields

$$\frac{\partial}{\partial x_l^m} \ln S_{x_m} = \sum_i \frac{\partial x_i^m}{\partial x_l^m} \ln S_i^m + \sum_i x_i^m \frac{\partial}{\partial x_l^m} \ln S_i^m. \tag{A.2}$$

Noting from Eq. (2.18) that

$$\ln S_i^m = \ln K_i^m Q_i^n - \ln x_i^m - \ln \lambda_i^m, \tag{A.3}$$

the first derivative is given by

$$\frac{\partial}{\partial x_l^m} \ln S_i^m = -\left(\frac{1}{x_i^m} \frac{\partial x_i^m}{\partial x_l^m} + \frac{\partial \ln \lambda_i^m}{\partial x_l^m}\right). \tag{A.4}$$

It follows that:

$$\sum_i x_i^m \frac{\partial}{\partial x_l^m} \ln S_i^m = -\sum_i x_i^m \left(\frac{1}{x_i^m} \frac{\partial x_i^m}{\partial x_l^m} + \frac{\partial \ln \lambda_i^m}{\partial x_l^m}\right), \tag{A.5}$$

$$= 0, \tag{A.6}$$

since according to the Gibbs–Duhem equation

$$\sum_i x_i^m \frac{\partial}{\partial x_l^m} \ln \lambda_i^m = 0, \tag{A.7}$$

and

$$\sum_i \frac{\partial x_i^m}{\partial x_l^m} = \delta_{il} - \delta_{iN_m}. \tag{A.8}$$

Thus

$$\frac{\partial}{\partial x_l} \ln S_{x_m} = \sum_i \frac{\partial x_i^m}{\partial x_l^m} \ln S_i^m, \tag{A.9}$$

$$= \ln \left(\frac{S_l^m}{S_{N_m}^m}\right). \tag{A.10}$$

Thus, the first derivative vanishes at a common intersection point S_m^* [see Eq. (2.20)]

$$\frac{\partial}{\partial x_l^m} \ln S_{x_m}\Big|_{S_m^*} = \sum_i \frac{\partial x_i^m}{\partial x_l^m} \ln S_m^*, \tag{A.11}$$

$$= \ln S_m^* \sum_i \frac{\partial x_i^m}{\partial x_l^m} = 0. \tag{A.12}$$

Conversely, if the first derivative is zero, the point is a common intersection point. From this result it follows that the saturation state S_{x_m} evaluated at S_m^* is either a maximum, minimum or inflection point. To evaluate stability, the second derivative is needed. It follows that:

$$\frac{\partial^2}{\partial x_l^m x_i^m} \ln S_{x_m} = \frac{\partial}{\partial x_l^m} \ln S_i^m - \frac{\partial}{\partial x_l^m} \ln S_{N_m}^m, \tag{A.13}$$

$$= -\frac{x_i^m + \delta_{il} x_{N_m}^m}{x_i^m x_{N_m}^m} - \frac{\partial}{\partial x_l^m} \ln \left(\frac{\lambda_i^m}{\lambda_{N_m}^m}\right). \tag{A.14}$$

For a binary solid solution with $x = x_1^m$

$$\frac{\partial^2}{\partial x^2} \ln S_{x_m}\Big|_{S_m^*} = -\frac{1}{x(1-x)} - \frac{\partial}{\partial x} \ln \left(\frac{\lambda_1}{\lambda_2}\right). \tag{A.15}$$

For an ideal binary solid solution, the second term on the right-hand side vanishes and the second derivative is always negative. This implies that the stoichiometric saturation state at the common end-member intersection point is a maximum. Consequently, an equilibrium point of a stoichiometric solid represents a true equilibrium state of the solid solution if and only if it is stable, i.e., the first derivative of the stoichiometric saturation vanishes and its second derivative is negative. Any other equilibrium point of the stoichiometric solid is unstable and therefore does not correspond to equilibrium of the solid solution.

For a non-ideal binary solid solution with solid activity coefficients given by the second order Guggenheim expansion with expansion coefficients α_0 and α_1

$$\ln \lambda_1(x) = (1-x)^2(\alpha_0 - \alpha_1(4x-1)), \tag{A.16}$$

$$\ln \lambda_2(x) = x^2(\alpha_0 + \alpha_1(3-4x)), \tag{A.17}$$

it follows that:

$$\frac{\partial}{\partial x} \ln \left(\frac{\lambda_1}{\lambda_2}\right) = -2(\alpha_0 + 3\alpha_1(1-2x)). \tag{A.18}$$

Depending on the sign and magnitude of the expansion coefficients α_0 and α_1, the sign of the second derivative may be positive or negative.

Appendix B. Generalized Lippmann diagrams

To visualize the relations between aqueous and solid compositions, Lippmann (1980) introduced an alternative approach which has the distinct advantage of enabling both the evolution of the solid and aqueous compositions to be followed on the same diagram, referred to as a Lippmann diagram (Glynn et al., 1990). For a multicomponent system the end-member mass action equations given in Eq. (2.4) are rearranged and summed over the ion activity product for all end members to determine the solidus (composition of the equilibrium solid)

$$\sum_i Q_i^m = \sum_i \frac{\lambda_i^m x_i^m}{K_i^m}. \tag{B.1}$$

Alternatively, solving Eq. (2.4) for x_i^m

$$x_i^m = \frac{K_i^m Q_i^m}{\lambda_i^m}, \tag{B.2}$$

and summing over all end members gives

$$\sum_i \frac{K_i^m Q_i^m}{\lambda_i^m} = 1. \tag{B.3}$$

Introducing the ion activity product fraction X_i^m defined by

$$X_i^m = \frac{Q_i^m}{\sum_{i'} Q_{i'}^m}, \tag{B.4}$$

determines the solutus

$$\sum_i Q_i^m = \frac{1}{\sum_i \frac{K_i^m X_i^m}{\lambda_i^m}}. \tag{B.5}$$

The Lippmann diagram is formed by graphing the logarithm of the right-hand sides of Eqs. (B.1) and (B.5) against x_i^m and X_i^m as independent variables. Thus

$$\mathcal{L}_m(x_m) = \log\left[\sum_i \frac{\lambda_i^m x_i^m}{K_i^m}\right], \tag{B.6a}$$

and

$$l_m(X_m) = -\log\left[\sum_i \frac{K_i^m X_i^m}{\lambda_i^m}\right], \tag{B.6b}$$

defining the solidus and solutus equations, respectively, where the shorthand notation $X_m = (X_1^m, \ldots, X_{N_m}^m)$ is used. Tie lines connect the solid and aqueous compositions at equilibrium

$$\mathcal{L}_m(x_m) = l_m(X_m). \tag{B.7}$$

Note that for non-ideal solid solutions the equation for the solutus depends on both aqueous and solid compositions through the solid activity coefficients λ_i^m. In general, to implement these relations it is necessary to obtain the solid solution composition x_i^m as a function of the aqueous solution composition mole fractions X_i^m which follows from the identity

$$\frac{\lambda_i^m x_i^m}{K_i^m X_i^m} = \sum Q_i^m. \tag{B.8}$$

Substituting the expression for the solidus from Eq. (B.1) for the right-hand side gives

$$X_i^m = \frac{\lambda_i^m x_i^m / K_i^m}{\sum_{i'} \lambda_{i'}^m x_{i'}^m / K_{i'}^m}. \tag{B.9}$$

For non-ideal solid solutions, calculation of the solutus requires determining $x_i^m = x_i^m(X_m)$. This is achieved by combining Eq. (B.9) with Eq. (B.5) where the right hand side is determined by the solidus given by Eq. (B.1).

References

Berthelot, M., 1872. On the law which governs the distribution of a substance between two solvents. *Ann. Chim. Phys.* **26**, 408–417, 4th series.

Doerner, H.A., Hoskins, W.M., 1925. Coprecipitation of radium and barium sulfates. *J. Am. Chem. Soc.* **47**, 662–675.

Ferry, J.M., Rumble, D., Wing, B.A., Penniston-Dorland, S.C., 2005. A new interpretation of centimetre-scale variations in the progress of infiltration-driven metamorphic reactions: case study of carbonated metaperidotite, Val d'Efra, Central Alps, Switzerland. *J. Petrol.* **46** (8), 1725–1746.

Glynn, P.D., Reardon, E.J., 1990. Solid-solution aqueous-solution equilibria: thermodynamic theory and representation. *Am. J. Sci.* **290**, 164–201.

Glynn, P.D., Reardon, E.J., Plummer, L.N., Busenberg, E., 1990. Reaction paths and equilibrium end-points in solid-solution aqueous-solution systems. *Geochim. Cosmochim. Acta* **54** (2), 267–282.

Guggenheim, F.A., 1952. *Mixtures*. Clarendon Press, Oxford.

Helgeson, H.C., 1968. Evaluation of irreversible reactions in geochemical processes involving minerals and aqueous solutions–I. Thermodynamic relations. *Geochim. Cosmochim. Acta* **32**, 853–877.

Lichtner, P.C., 2001. *FLOTRAN User Manual, LA-UR-01-2349*. Los Alamos National Laboratory, Los Alamos, New Mexico.

Lichtner, P.C., 1993. Scaling properties of kinetic mass transport equations. *Am. J. Sci.* **293**, 257–296.

Lichtner, P.C., 1990. The quasi-stationary state approximation to fluid/rock reaction: local equilibrium revisited. In: Ganguly, J. (Eds.), *Advances in Physical Geochemistry*, vol. 8, pp. 452–560.

Lichtner, P.C., 1988. The quasi-stationary state approximation to coupled mass transport and fluid-rock interaction in a porous medium. *Geochim. Cosmochim. Acta* **52**, 143–166.

Lichtner, P.C., 1985. Continuum model for simultaneous chemical reactions and mass transport in hydrothermal systems. *Geochim. Cosmochim. Act* **49**, 779–800.

Lichtner, P.C., Steefel, C.I., Oelkers, E.H., 1996. Reactive transport in porous media. *MSA Rev. Mineral.* **34**, 438.

Lippmann, F., 1980. Phase diagrams depicting aqueous solubility of binary mineral systems. *Neues Jahrb. Mineral. Abteil.* **139**, 1–25.

Murphy, W.M., Smith, R.W., 1988. Irreversible dissolution of solid solutions: a kinetic and stoichiometric model. *Radiochim. Acta* **44/45**, 365–401.

Nernst, W., 1891. Distribution of a substance between two solvents and between solvent and vapor. *Phys. Chem.* **8**, 110–139.

Nordstrom, D.K., Munoz, J.L., 1985. *Geochemical Thermodynamics*. Benjamin/Cummings, Menlo Park, CA, 477 pp.

Nourtier-Mazauric, E., Guy, B., Fritz, B., Brosse, E., Garcia, D., Clément, A., 2005. Modelling the dissolution/precipitation of ideal solid solutions. *Oil Gas Sci. Technol.—Rev. IFP* **60** (2), 401–415.

Parkhurst, D.L., Appelo, C.A.J., 1999. User's guide to PHREEQC–A computer program for speciation, reaction-path, advective-transport, and inverse geochemical calculations: U.S. Geological Survey Water-Resources Investigations Report 95-4227, 143 p.

Prigogine, I., Defay, R., 1969. *Chemical Thermodynamics*. Longmans, 543 pp.

Sack, R.O., 2005. Internally consistent database for sulfides and sulfosalts in the system Ag_2S–Cu_2S–ZnS–FeS–Sb_2S_3–As_2S_3: Update. *Geochim. Cosmochim. Acta* **69** (5), 1157–1164.

Sack, R.O., Fredericks, R., Hardy, L.S., Ebel, D.S., 2005. Origin of high-Ag fahlores from the Galena Mine, Wallace, Idaho, USA, *Am. Mineral.*, **90**, 1000–1007.

Wolery, T.J., 1992. EQ3/6, A Software Package for Geochemical Modeling of Aqueous Systems. Package Overview and Installation Guide. (Version 7.0) UCRL-MA-110662-PTI. Livermore, California: Lawrence Livermore National Laboratory.